Thymic selection of the T cell receptor repertoire is biased toward autoimmunity in females

Hélène Vantomme[1,2], Valentin Quiniou[1], Leslie Adda[1§], Charline Jouannet[1§], Vanessa Mhanna[1§], Céline Albalaa[1$], Pierre Barennes[1$], Nicolas Coatnoan[1,2$], Vimala Diderot[1,2$], Johanna Dubois[1$], Gwladys Fourcade[1$], Kenz Le Gouge[1$], Otriv Frédéric Nguekap Tchoumba[1$], Martin Pezous[1$], Paul Stys[1$], Adrien Six[1], Encarnita Mariotti-Ferrandiz[1,3]* and David Klatzmann[1,2*#].

[§]contributed equally, alphabetical order

[$]contributed equally, alphabetical order

*co-senior authors

[#]corresponding author

1. Immunology, Immunopathology, Immunotherapy i3 Lab, INSERM UMRS-959, Sorbonne Université, Paris, France
2. Biotherapy (CIC-BTi) and Inflammation-Immunolopathology-Biotherapy Department (i2B), Assistance Publique -Hôpitaux de Paris (AP-HP), Paris France
3. Institut Universitaire de France

Corresponding author :
Prof. David KLATZMANN MD, PhD
I3 Lab (Immunology Immunopathology Immunotherapy) INSERM UMRS 959 – Sorbonne Université
Bâtiment CERVI, GHPS Pitié-Salpêtrière, 83 boulevard de l'Hôpital, 75013 Paris, France
Tel : +33 1 42 17 74 61
Email : david.klatzmann@sorbonne-universite.fr

The authors have declared that no conflict of interest exists.

Abstract: (200 words)

Women represent about 80% of patients with autoimmune diseases. This may partly result from sex-based differences in T cell receptor (TCR) selection during thymocyte development, potentially influenced by hormones and the lower expression of the Autoimmune Regulator (AIRE) transcription factor in females.

To investigate this, we analyzed sex-specific differences in TCR generation and selection. We examined TCR repertoires in double-positive thymocytes and single-positive thymic cells, including $CD8^+$ and $CD4^+$ effector T cells and regulatory T cells (Tregs), derived from male and female organ donors. Minimal sex-based differences were observed in V and J gene usage, and there were no notable differences in TCR repertoire diversity, complementarity-determining region 3 (CDR3) length, amino acid composition, or network structure. No TCR sequences were exclusive to either sex.

However, female effector T cells exhibited a significantly higher prevalence of TCRs specific to self-antigens implicated in autoimmunity compared to males, while female Tregs showed a reduced frequency of such TCRs. These differences were not observed for TCRs targeting self-antigens unrelated to autoimmunity or antigens associated with cancer or viruses.

Our findings identify a sex-specific imbalance in thymic selection of TCRs with autoimmunity-associated specificities, providing mechanistic insight into the increased susceptibility of women to autoimmune diseases.

55 ## Introduction

56 Several studies have highlighted a sex imbalance in diseases involving the immune system.
57 This is particularly evident in the case of autoimmune diseases (AIDs), where 80% of affected
58 individuals are women, and the severity of the condition varies between the sexes (1–3). In
59 addition, men are more severely affected by infectious diseases such as COVID-19 and
60 tuberculosis (4,5). The response to preventive immunotherapies such as vaccination, and to
61 curative treatments, like immune checkpoint inhibitors or anti-TNF alpha, is also sex
62 dependent (6). These observations indicate the presence of intrinsic biological differences in
63 immune responses between males and females.

64 A variety of factors have been identified that could help explain the observed sex-based
65 differences. Among these, sex hormones have been shown to influence immune responses
66 by acting on immune cells that express specific receptors to these hormones (7–9). Sex
67 hormones could directly influence the adaptive immune response at the level of thymocyte
68 differentiation and selection by acting on the expression of Autoimmune Regulator (AIRE) in
69 thymic epithelial cells. AIRE is responsible for the thymic expression of otherwise tissue-
70 specific antigens, contributing to both the negative selection of effector cells and the positive
71 selection of Tregs that recognize such antigens (10). Research has shown that testosterone
72 increases AIRE expression in medullary thymic epithelial cells, whereas estradiol decreases it
73 (11,12). Furthermore, a recent study has shown that the transcriptomic profiles of these
74 specialized antigen-presenting cells in the thymus differ between males and females (13). This
75 suggests that there may be differences in the selection of the T cell receptor (TCR) repertoire
76 between males and females.

77 Despite these findings, there is still limited knowledge about potential differences in the TCR
78 repertoire between the sexes. The generation of the TCR is a key process in T-cell
79 development that takes place in the thymus. The TCR consists of two chains, alpha (TRA) and
80 beta (TRB), each of which resulting from a random genetic rearrangement involving the V
81 (variable), D (diversity) [for the TRB], and J (joining) genes. The combination of these gene
82 segments is accompanied by insertions and deletions, creating a highly diverse region, the
83 Complementarity Determining Region 3 (CDR3) (14). It is this region of the TCR that
84 predominantly interacts with the peptide, a critical interaction for antigen recognition and
85 subsequent T cell activation. The ability to specifically recognize diverse antigens via the CDR3
86 is central to the efficiency and specificity of the adaptive immune response.

87 TCRs are randomly generated, which means that while some may be useful, others may be
88 harmful by recognizing self-antigens and causing autoimmunity. The current understanding is
89 that during thymocyte development, selection is based on the avidity of their TCRs for
90 antigens presented by cortical and medullary thymic epithelial cells. Thymocytes expressing
91 TCRs with insufficient avidity fail to receive survival signals and undergo death by neglect
92 during positive selection, whereas those with excessive avidity are actively eliminated via
93 negative selection to ensure self-tolerance. In contrast, thymocytes with intermediate avidity
94 are positively selected and mature into single-positive cells, either CD4+ or CD8+. Thymocytes
95 with the highest of these intermediate affinities develop in Tregs. Given AIRE's pivotal
96 function in these processes, sex differences in AIRE expression may significantly influence
97 thymic selection.

98 The TCR repertoire of female and male peripheral T cells have shown that their diversity,
99 particularly that of the TRB repertoire, is influenced not only by the age of the individuals but

100 also by their sex (15–18). However, another study showed no association between the sex of
101 individuals and the diversity of their TCR repertoire (19). Nevertheless, the study of peripheral
102 blood TCRs reflects that of an immune system that has undergone multiple immune
103 responses. For example, observed differences between males and females in their responses
104 to self-antigens associated with autoimmunity could indicate either the cause (the TCRs drive
105 the disease) or the consequence (the TCRs are expanded because of the disease).

106 To assess whether there are significant differences in the generation and thymic selection of
107 the TCR repertoire between males and females, we therefore focused on analyzing the TCR
108 repertoires of thymocytes. These cells represent the latest stage in T cell development and
109 have not yet been involved in immune responses. Their repertoires thus represent the
110 mechanisms of TCR generation for the analysis of CD4/CD8 double positive (DP) cells, and of
111 TCR selection for CD4 and CD8 simple positive (SP) T cells. We generated a unique data set
112 comprising the sequences of the TRA and TRB chains of DP cells, CD8 and CD4 SP effector
113 cells, and CD4 SP Tregs from organ donors, both infants and adults. The analysis of TRA and
114 TRB repertoires using state-of-the-art strategies revealed no sex differences in repertoire
115 generation (DP cell repertoire), but an enrichment in females for CD8 SP T cells bearing CDR3
116 associated with specificities related to autoimmunity.

117 # Results

118 We analyzed thymic TCRαβ repertoires from 22 human organ donors (11 females, 11 males,
119 aged between 73 days and 64 years) (**Figure 1, Supplementary Figure 1**). For each donor,
120 CD3+CD4+CD8+ double positive (DP), CD3+CD4-CD8+ CD8 single positive (SP), and
121 CD3+CD4+CD8- CD4 SP thymocytes were sorted by flow cytometry. In 16 donors, CD4 SP
122 cells were further subdivided into CD25- conventional CD4 Teff and CD25+ CD4 Treg
123 subsets, whereas in the remaining six donors, total CD4 SP cells were analyzed as Teff-
124 enriched populations. This resulted in 20 DP, 21 CD8 SP, 22 CD4 Teff SP and 14 CD4 Treg SP
125 samples (**Figure 1, Supplementary Figure 1**). Bulk TCR sequencing was then performed on
126 each cell subset, with the aim to characterizing the TRA and TRB repertoires. Rank–
127 frequency plots of clonotype abundances displayed comparable heavy-tailed distributions
128 across donors, without any obvious systematic differences between males and females
129 (**Supplementary Figure 2**).

130 ## Minimal sex-based differences in TCR V and J gene usage across thymic cell
131 subsets.

132 The first level of diversity in generating TCRs is the usage of V and J genes (20). We analyzed
133 the usage of TRA and TRB V and J genes and their combinations in each thymocyte population
134 (**Figure 1**).

135 Males and females had a relatively similar V gene usage, as evidenced by the lack of a clear
136 separation in the Principal Component Analysis (PCA), for both TRA and TRB, and across all
137 cell subtypes studied (**Figure 2A**). However, we observed some individual differences in V and
138 J gene usage between males and females, with some being specific to certain cell subtypes
139 (**Supplemental Figures 3-6**), and others observed across multiple cell subtypes (**Supplemental**
140 **Figures 3-6**). For example, TRBV6-5 was found to be more highly expressed in females

141 compared to males in DP cells (**Supplemental Figure 3C**) and CD8 SP cells (**Supplemental**
142 **Figure 4C**).
143 In the following step, we compared the usage of TRAV-TRAJ and TRBV-TRBJ gene
144 combinations across all individuals using the Jensen-Shannon Divergence (JSD) score (**Figure**
145 **2B**). The hierarchical clustering showed no clear separation between male and female
146 individuals for any of the chain or cell subtype, indicating no significant differences in the gene
147 combination usage between males and females (**Figure 2B**). A similar observation was made
148 when directly analyzing the frequency of these V-J gene combinations (**Supplemental Figures**
149 **3E-6E, 3F-6F**).

150 Comparable TCR repertoire diversity between males and females

151 A high diversity of the TCR repertoire is essential for generating a broad potential reactivity
152 against a variety of antigens. We thus compared the TCR repertoire diversity between males
153 and females. To achieve this objective, we analyzed Rényi diversity curves (from zero to
154 infinite α parameters) that measure various aspects of TCR repertoire diversity. At different
155 α values, the Rényi index places more or less weight on the contribution of the most frequent
156 clonotypes. Higher α values highlight the most prevalent clonotypes, thereby revealing the
157 effect of expanded clones on overall diversity.
158 Rényi curves showed comparable diversities between sexes in DP and CD4 Teff cells, for both
159 TRA and TRB, and a difference in CD8 and CD4 Treg cells (**Supplemental Figure 7**). In CD8 cells,
160 the curves begin to diverge at low α values (**Supplemental Figure 7**), with an earlier inflection
161 in males, indicating a less balanced distribution of TCR clones. This suggests that in males,
162 fewer clones dominate the repertoire at lower diversity thresholds compared to females. In
163 Tregs, while the inflection point is similar, the difference seems to be characterized by higher

164 diversity and richness in females compared to males (**Supplemental Figure 7**). However, no
165 significant differences were observed for the Shannon diversity index (α = 1), the Simpson
166 index (α = 2), and the Berger-Parker index (α = infinite), for both chains and all cell subtypes
167 (**Figure 3**). These results indicate that the diversity of thymic TCR repertoire is similar between
168 males and females.

169 Comparable CDR3aa length distribution in male and female TCR repertoires

170 Most of the repertoire diversity is generated by the random addition of nucleotides within
171 the VDJ junctions, resulting in the hypervariable CDR3 region that interacts with the peptide-
172 MHC complex, and is mostly responsible for the TCR specificity. The CDR3 length has been
173 shown to directly influence the TCR's ability to interact with the peptide (21). We thus studied
174 the distribution of CDR3 aa (CDR3aa) sequence lengths between males and females to identify
175 potential TCR generation and/or selection biases (**Figure 1**).
176 Our results showed that males and females have a comparable distribution of CDR3aa lengths
177 for both TRA (**Supplemental Figure 8**) and TRB (**Figure 4A**). CDR3aa sequences in TRA were
178 shorter than those in TRB, as previously described in peripheral blood T cells (22,23). Although
179 there were subtle differences in certain CDR3aa lengths between males and females, these
180 variations were minimal, involving sequences that represent less than 2% of the total TCR
181 repertoire (**Figure 4A** and **Supplemental Figure 8**). Altogether, the overall distribution of
182 CDR3aa length is comparable between males and females.

183 Subtle differences in the composition of CDR3aa in the thymic TCR repertoires
184 of males and females.

185 We analyzed the aa usage within the FG loop of the CDR3, which is in contact with the peptide-
186 MHC complex (24). The classification of aa was determined based on their hydropathy

187 properties, categorized as follows: hydrophilic, hydrophobic, or neutral (25). We observed
188 significant differences in the usage of some aa between males and females for both TRA
189 (**Supplemental Figure 9**) and TRB (**Figure 4B**). In DP cells, these differences predominantly
190 involved hydrophobic aa: females exhibited higher alanine (A) usage in TRA and lower in TRB
191 compared with males (**Figure 4B** and **Supplemental Figure 9**). Additionally, females showed
192 increased usage of phenylalanine (F) and isoleucine (I) in TRB (**Figure 4B**). Furthermore, other
193 aa with varying hydropathy properties were differentially used between males and females
194 in CD4 Teff and Treg populations (**Figure 4B** and **Supplemental Figure 9**).
195 We then examined the usage of aa specifically at positions p109 and p110 of the TRB CDR3aa
196 region, as hydrophobic aa at these two positions have been associated with a stronger
197 recognition of self-antigens (26–28). For each individual, we calculated the proportion of
198 unique TRB CDR3aa carrying a hydrophobic aa (excluding alanine, which is only weakly
199 hydrophobic) at these two positions. This positional analysis revealed a significant increase in
200 the usage of hydrophobic amino acid at position p109 in female CD8 cells compared with
201 males, with similar trends observed at p109 in DP and CD4 Teff subsets and at p110 in CD8
202 cells (**Figure 4C**). Taken together, these positional patterns suggest a subtle sex-biased
203 enrichment of hydrophobic amino acids at key TRB CDR3 positions that could be compatible
204 with a slightly increased potential for self-reactivity and cross-reactivity in female CD8 T cells
205 (28).

206 Slight sex-based variations in thymic TCR generation probability distribution.

207 Another approach to evaluating biases in the generation and selection of the TCR repertoire
208 is to compare the probability of generation (Pgen) of CDR3 nucleotide sequences (**Figure 1**).
209 Pgen represents the likelihood of a sequence being produced, according to models of V(D)J

210 recombination (14,29). For DP and CD8 cells only and for each TCR chain, a sequence
211 generation model was created using 100,000 non-productive nucleotide sequences. Using
212 this model, the Pgen of all productive TCR sequences that make up each repertoire was
213 calculated.
214 When comparing the distribution of Pgen between males and females, we observe a very
215 slight difference of distribution, characterized by a nearly null Kolmogorov-Smirnov score (D_{K-}
216 $_{S} < 0.05$) (**Figure 5**). This difference is more pronounced in the TRB compared to the TRA chain
217 (**Figure 5**). As this minor discrepancy might be indicative of variations among individuals
218 irrespective of their sex, we have generated 20,000 permuted mixed-sex groups utilizing our
219 dataset. Our findings revealed a significant distribution difference of Pgen sequences
220 between these mixed groups population (DP – TRA: $D_{K-S} = 0.0183 \pm 0.0145$ ($\mu \pm sd$), DP –
221 TRB: $D_{K-S} = 0.0190 \pm 0.0161$, CD8 – TRA: $D_{K-S} = 0.0227 \pm 0.0153$, and CD8 – TRB: $D_{K-S} = 0.0259$
222 ± 0.0140). However, the observed difference in the Pgen distribution between males and
223 females is higher than that between the mixed groups in the DP TRB.

224 Similar network structure of thymic TCR repertoires in males and females

225 Next, we evaluated whether thymic selection in males and females is directed towards similar
226 or distinct sequences. For each TCR repertoire, CDR3aa sequences are connected if they differ
227 by one aa, i.e. have a Levenshtein distance of =1 (**Figure 1**). Such linked sequences have a high
228 probability of sharing the same specificities (30). A random downsampling process to the
229 smallest sample was performed to compare samples of comparable sizes. This process was
230 repeated 100 times, and the results are detailed in the **Supplementary Table 1**. The shapes
231 of the network are depicted in **Figure 6A**.

232 To analyze these clusterings with greater precision, we used various metrics. When comparing
233 the number of clustered sequences in each individual network between males and females,
234 no significant differences were observed for any cell type in either chain (**Figure 6B**). Similarly,
235 the degree of sequence similarity, as indicated by the density of edges between sequences
236 within an individual's TCR repertoire, was comparable between males and females (**Figure**
237 **6C**). These findings indicate that there are no significant sex-specific differences in the
238 similarity of CDR3aa sequences, suggesting that males and females produce CDR3aa
239 sequences with the same degree of variability within their TCR repertoires.

240 Absence of sex-specific CDR3aa motifs in thymic TCR repertoires of males and 241 females

242 We then sought to determine whether we could detect CDR3aa sequence motifs that were
243 more prevalent in one group compared to the other, in order to evaluate whether the
244 selection of CDR3aa was biased towards particular sequences differently between males and
245 females (**Figure 1**). To identify sequences with shared characteristics that might indicate a
246 probable common specificity among individuals of the same group, the analysis focused
247 exclusively on CDR3aa sequences of the TRB, as this region has been shown to have a greater
248 influence on TCR specificity (31,32). Local motifs were defined using Gliph2 (33), which are a
249 sequences of three to five aa, as well as global motifs, which are sequences of more than
250 three aa where, at one position, an aa can be substituted by another aa if it has a positive
251 BLOSUM62 score (34). Importantly, only motifs containing public CDR3aa sequences shared
252 by at least two individuals were retained, thereby excluding private or individual-specific
253 sequences from the analysis.
254 We identified several hundred motifs that were differentially expressed between males and
255 females for each cell subpopulation. A greater number of motifs were specific to females,

256 ranging from 426 motifs for DP to 278 motifs for CD4 Tregs, compared to males, ranging from
257 328 motifs for CD4 Teffs to 34 motifs for CD4 Tregs (**Figure 7A**). The identified motifs are
258 mainly local motifs and largely confined to their respective sex group, indicating that motifs
259 identified in females are predominantly found in females, and vice versa (**Supplemental**
260 **Figure 10-13**).
261 As illustrated in **Figure 7B**, we observed minimal motif overlap between different cell
262 subtypes. Only two female associated motifs overlapped: one between CD4 Teffs and CD4
263 Tregs, and another between CD4 Teffs and CD8 cells (**Figure 7B**). In contrast, no overlap was
264 found between male-associated motifs (**Figure 7B**). Furthermore, it was observed that there
265 was an overlap between one motif associated with female CD8 cells and a motif associated
266 with male CD4 Teff cells (**Figure 7B**).
267 We then proceeded to evaluate the usage of the differentially expressed motifs in external
268 datasets. There is no publicly available thymic TCR dataset that reports repertoires according
269 to cell subsets. We thus tested these motifs on TCRs from pediatric bulk thymocytes, which
270 contains TCR data from children aged between two and eight months, with a male-to-female
271 ratio of 5:3 (35,36). We calculated the usage of these differentially expressed motifs in each
272 sample of this dataset. We were unable to separate individuals by sex using these motif
273 usages (**Figure 7C**).
274 We then evaluated these motifs using a peripheral blood TCR dataset from healthy
275 individuals, where CD8, CD4 Teff, and CD4 Treg cells had been sorted. The usage of these
276 motifs could not distinguish males from females across all cell subsets (**Figure 7D** and
277 **Supplemental Figure 14**).

278 **Sex-biased enrichment of TCRs associated with autoimmune diseases and**
279 **bacterial antigens.**

280 We sought to identify the usage of TCRs with known specificity as represented in the IEDB,
281 Mc-PAS and VDJdb public databases (37–39). We compiled the TCRs from these three
282 databases, retaining only those with high sequence reliability scores (see Materials and
283 Methods). We focused on TRB sequences exclusively, due to their greater representation in
284 the databases (31,40). We identified 55,368 unique TRB CDR3aa sequences with high
285 reliability and specificity assignment scores for at least one specificity.

286 We classified the TCR specificities based on the antigen they recognize: viral or bacterial
287 peptides, or human peptides overexpressed in cancers, autoimmune diseases (AIDs), or
288 neither of these diseases (**Supplemental Figure 15A**). We sought to identify the TRB CDR3aa
289 sequences in our thymocyte dataset. Depending on the individuals and cell subtypes, they
290 represented between 0.82% and 3.58% of the TRB repertoires.

291 We observed that unique TRB CDR3aa sequences specific to self-antigens not associated with
292 pathologies and those associated with cancers, are proportionally more represented in our
293 thymic TCR dataset than in the pooled reference database, in both females and males
294 (**Supplemental Figure 15B**). This pattern was consistent across all cell subtypes
295 (**Supplemental Figure 15B**). These comparisons to the reference database are presented for
296 descriptive purposes only, as differences between an experimental thymic repertoire and a
297 curated database are expected given the structure of the reference resource. We then
298 compared the distribution of these CDR3aa between males and females for each cell subtype.
299 Strikingly, in the TCR repertoires with one specificity only, we observed a significantly higher
300 proportion of unique TRB CDR3aa sequences associated with AIDs in female CD8 SP cells
301 compared to male CD8 SP cells (**Figure 8A**). Furthermore, in the specific TCR repertoires only,

302 there was a trend towards a higher proportion of thymic sequences with specificity associated
303 to bacterial compounds in female CD8 SP cells compared to males, and an opposite trend was
304 observed for CD4 Tregs SP (**Figure 8A**). These differences observed in CD8 SP cells persisted
305 when examining the usage of these sequences (i.e. cumulative usage frequency), with
306 significantly higher usage of sequences with specificity associated to bacterial compounds and
307 those associated with AIDs in females compared to males (**Figure 8B**). Of particular note are
308 the donor-resolved analyses (**Supplementary Figures 15B and 16**), in which each individual is
309 represented separately. These confirm that these patterns are not driven by a single donor.
310 Donor age had no significant effect on the sex-biased enrichment of self- and bacteria-specific
311 TRB CDR3 sequences in CD8 SP and CD4 Treg SP cells ($p \geq 0.52$), indicating that the observed
312 differences are age-independent (**Supplemental Figure 17**). In addition, we investigated for
313 the presence of polyspecific TCRs, which are capable of recognizing multiple antigens from
314 different organisms (41–43). These sequences were found to be enriched across all cell
315 subtypes, in comparison to their representation in the reference database (**Supplemental**
316 **Figure 15C**). However, no significant differences were observed in the proportion or usage of
317 these polyspecific sequences between males and females. Interestingly, an inverse usage
318 trend was observed between CD8 and CD4 Treg SP cells: females exhibited higher usage of
319 these sequences in the CD8 SP repertoire but a lower usage in the CD4 Treg SP repertoire
320 compared to males (**Figure 8C-8D**).
321 In conclusion, our analysis of TCR specificity has identified sex-specific differences in the
322 thymic selection of CD8 effector T cells associated to autoimmune and bacterial antigens that
323 are overrepresented in female versus males.

324 ## Discussion

325 It is noteworthy that there is a paucity of research on potential differences in the TCR
326 repertoire between the sexes, despite the much higher prevalence of autoimmune diseases
327 in females, a topic that remains to be fully elucidated. To explore the hypothesis that the
328 generation and/or the selection of the TCR repertoires may be different between sexes
329 requires, it is necessary to study the TCR repertoire where they are formed and selected, in
330 the thymus. We thus generated a unique and valuable dataset comprising thymic samples
331 collected from deceased organ donors of various ages, and young children who have
332 undergone cardiac surgery. Firstly, we separated the various thymocytes populations in order
333 to study both TCR repertoire generation at the level of DP cells, and repertoire selection at
334 the level of CD8, CD4 Teff and Treg SP cells. We performed bulk sequencing of the TCRs from
335 these cells, as this is the only method that yet generates enough sequences for sensitive
336 comparison at this time. Single-cell sequencing is an analyzing technique that it is limited in
337 its scope. It is only capable of analyzing a few thousand cells and would not have enabled the
338 analyses that can be performed with hundreds of thousands of cells.

339 **TCR generation**

340 Our analyses initially revealed similarities rather than dissimilarities in TCR generation. Our
341 detailed analyses revealed no significant sex differences in relation to the majority of the
342 examined variables when comparing males and females DP cells' repertoires, except for
343 differences in the usage of small number of V and J genes from both TCR chains. However,
344 these minor discrepancies are likely attributable to random variation, considering the
345 extensive number of comparisons conducted. This finding is further supported by the
346 observation that there are no significant differences in the usage of TRBV-TRBJ and TRAV-
347 TRAJ gene associations between males and females. We also observed no differences in

348 diversity indexes in DP cells' repertories between males and females. Altogether, the overall
349 combinatorial diversity of the TCR repertoire remains comparable between sexes.
350 A detailed analysis of the CDR3aa region in DP cells showed that some hydrophobic aa in the
351 FG loop region are differently found for both TCR chains. However, no significant sex-based
352 differences were found in the usage of hydrophobic aa at the critical p109 and p110 positions
353 in TRB that have been described as influencing self-antigen recognition due to the impact of
354 hydrophobic aa on TCR self-reactivity (26–28). These findings suggest that the subtle sex-
355 based differences in the FG loop's aa usage are minor and do not significantly impact the
356 overall characteristics of the CDR3 region in a sex-dependent manner.
357 The Pgen analysis of DP cells revealed only minimal differences in the distribution of Pgen
358 between males and females, which were similar to those observed in control groups. This
359 indicates that the mechanisms governing TCR generation are largely consistent across sexes,
360 with only minor, likely random, deviations.
361 Additionally, although we identified TRB CDR3aa sequence motifs that were differentially
362 expressed between males and females at the DP cell stage in our dataset, these motifs could
363 not reliably differentiate individuals by sex in external datasets. This indicates that they are
364 more dataset-specific than sex-specific. This issue may also be explained by the different
365 characteristics of our data and that of the other dataset. For example, in the Arstila dataset,
366 the analyses were performed on unsorted cells from young subjects. Younger individuals tend
367 to have a more diverse and richer TCR repertoire, with greater repertoire sharing in the
368 periphery, which could potentially obscure sex-specific patterns (16,44). This suggests that
369 these motifs might be context-specific or influenced by other factors such as age, genetic
370 background, or environmental exposures. Moreover, we did not observe any sex-specific

371 differences in CDR3 TRB specificity usage in DP cells' repertoires. In summary, our results from
372 DP cells analyses could not identify any relevant sex differences in TCR generation.

373 **TCR selection**

374 We identified three genes that show differential usage between males and females. Whilst it
375 is possible that some of these differences are merely random, resulting from multiple
376 comparisons, the preferential use of TRBV6-5 in females has previously been observed in the
377 peripheral TCR repertoire (45). Notably, this gene is overrepresented in female lupus patients
378 compared to their controls (51,52). Although the preferential usage of TRBV6-5 in females is
379 consistent with previous peripheral observations, external validation of this thymic bias
380 remains challenging. Publicly available TCR datasets rarely provide (i) sorted thymocyte
381 subsets, (ii) balanced sex representation, and (iii) sufficient sequencing depth within each
382 subset to allow reliable comparison of gene usage patterns. Moreover, differences in tissue
383 origin (peripheral blood versus thymus), age distribution, and technical protocols may
384 substantially influence TRBV usage frequencies. For these reasons, direct replication in
385 independent thymic cohorts is currently not feasible. Our permutation-based internal control
386 analysis was therefore implemented to ensure that the observed signal was not attributable
387 to random donor grouping or individual-level variation.

388 Our most striking observation relates to significant sex-specific differences in inferred
389 specificities of CD8 T cells, with a biased CD8 selection process in the thymus favoring
390 sequences associated with autoimmune diseases and bacterial antigens in females. The fact
391 that this bias does not affect DP cells indicates that it is related to TCR selection rather than
392 generation. Its relevance is strongly supported by the fact that (i) there is no such bias for
393 other self-antigens that are not associated with autoimmunity and (ii) the bias affects both
394 the effectors and regulators of autoimmunity with a directionality compatible with the

395 increased prevalence of autoimmune disease in females. TCRs associated with autoimmunity-
396 related self-antigens have been observed to be increased in CD8 effector T cells, while
397 decreased levels have been seen in CD4 Tregs. It should be noted that this bias also affects
398 certain bacterial antigens, though not viral antigens. This phenomenon could be explained by
399 the fact that bacterial antigens express numerous mimotopes of self-antigens, and are known
400 to contribute to the shaping of the TCR repertoire. The observed bias towards bacterial
401 antigens in female CD8 T cells could also provide more effector cells specific for bacterial
402 antigens that mimic self-antigens, contributing to autoimmune disease development by
403 molecular mimicry (48). In this line, antigens linked to celiac disease (CeD) and type 1 diabetes
404 (T1D) are highly represented in the database and these two AIDs have been linked to bacterial
405 components that may mimic self-antigens (49–53). As is well-established, the gut microbiota
406 influences thymic development of T cells (54). Sexual hormones could influence this biased
407 selection by affecting the composition of the gut microbiota (55) and/or by affecting the
408 selection of the TCRs specific for these antigens. In addition to these specific patterns, we
409 observed a significant increase in the usage of hydrophobic amino acids at the central p109
410 position of the TRB CDR3aa in female CD8 thymocytes, with similar trend at p110.
411 Hydrophobic residues at these positions have been implicated in enhanced self-reactivity and
412 cross-reactivity of CD8 T cells (26–28), suggesting that female CD8 thymocytes may be slightly
413 enriched for TCRs with intrinsically higher potential for recognizing self-like or cross-reactive
414 peptide MHC complexes. It is noteworthy that the positional hydrophobicity of CD8 T cells
415 CDR3s is consistent with the over-representation of sequences annotated as recognizing
416 autoimmune-associated self-antigens, pointing to a more autoreactive TCR repertoire.
417 Finally, we have recently described polyspecific TCRs that can respond to multiple unrelated
418 viral antigens and hypothesized their possible involvement in autoimmunity (43). We defined

419 a CDR3 as being polyspecific if the TCRs containing it have been experimentally associated
420 with epitopes from at least two different antigen origins. We observed a higher usage of
421 polyspecific sequences in the CD8 SP repertoire of females, although this was not statistically
422 significant. In contrast, the frequency of polyspecific TCR sequence usage was lower in female
423 CD4 Tregs SP cells. These observations, which could be indicative of improved anti-infectious
424 responses and worse autoimmune responses in women, warrant further exploration.
425 These inferences rely on a harmonized specificity compendium combining McPAS-TCR, IEDB
426 and VDJdb, which provide complementary and only partially overlapping landscapes
427 (pathology-enriched versus predominantly viral specificities). Although there is limited
428 numerical overlap between our thymic repertoires and annotated sequences is limited, this
429 is to be expected given that public databases currently capture only a small fraction of the
430 potential TCR specificity space. In this context, the sex-biased enrichment of sequences
431 annotated as autoimmune- and bacteria-associated should be viewed as a robust signal
432 emerging from a very sparse annotation space. However, it should still be interpreted as
433 hypothesis-generating rather than exhaustive.
434 To further evaluate the robustness of our findings, we performed additional analyses to
435 assess whether donor age could confound the observed sex-specific differences. A potential
436 limitation of our study is the relatively wide age range of donors. However, the absence of
437 distinct age-related clustering in repertoire features, the lack of age impact on CD8 and CD4
438 Treg bacterial-specific TRB usage and CD8 and CD4 Treg self-associated to autoimmune
439 disease-specific TRB usage patterns (Supplemental Figure 17), argue against age as a
440 confounding factor. These results support the hypothesis of an intrinsic sex bias in thymic TCR
441 selection rather than an age-related effect.

442 While our findings provide valuable insights into sex-specific differences in thymic selection
443 of TCR repertoires, our TCR specificity analyses were limited. We can confirm that our study
444 focused exclusively on the TRB CDR3aa region of the TCR, which is widely acknowledged as
445 the most critical element in defining TCR specificity (31,32) while both the TRA and the TRB
446 chains contribute to TCR specificity (31,32). This limitation is intrinsic to the limited number
447 of TRA with assigned specificity in databases and to the fact that, given the nature of our
448 studies, there is a need to study large repertoires, which is currently not feasible by single cell
449 TCR sequencing. However, as methods for inferring specificity continue to evolve, they will
450 likely allow more refined analyses of our dataset in the future (56). Furthermore, the
451 continuous development of the TCR database should enhance these analyses.
452 Despite the relatively small size of our cohort, which was outbred, we believe that this design
453 is essential for capturing sex-associated differences. Inbred models would reduce inter-
454 individual variability, but they would not reflect the complexity of human thymic selection,
455 nor the interplay between sex and genetic diversity. Despite the modest sample size, the
456 consistency of the observed patterns across the analytical approaches supports the
457 robustness of our conclusions.
458 Altogether, our analyses of TCR specificity identified a biased selection in females towards
459 sequences associated with autoimmune diseases, supporting the idea that early central
460 tolerance mechanisms may represent one layer contributing to sex differences in
461 autoimmune susceptibility, in interaction with peripheral and environmental factors. Future
462 research should focus on validating these observations in relevant independent datasets,
463 which are currently lacking.
464

465 # Methods

466 ### *Samples*

467 Thymus samples were obtained from twenty-two organ donors aged between 73 days and 64
468 years, without any specific pathologies (**Figure 1**). Individual partial HLA typing is detailed in
469 **Supplementary Table 2**. Adult samples were collected post-surgery at the Cardiac Surgery
470 Departments of many hospitals in France, following approval by the Agence de Biomédecine
471 and the Ministry of Research (#PFS14-009). Pediatric samples were obtained following total
472 thymectomy during cardiac surgeries at Necker Hospital. The ratio of male to female across
473 donors is maintained at 1:1, although it varies between 1.1:1 and 1.33:1 depending on the
474 cell subtypes analyzed. The age distributions of male and female donors were compared using
475 two-sample Kolmogorov–Smirnov tests, with no significant differences observed across
476 thymic subsets ($p > 0.46$), indicating no age-related confounding (**Supplementary Figure 1**).

477 ### *Thymocyte isolation and RNA extraction*

478 Thymic cell suspensions were prepared through automated tissue dissociation using
479 gentleMACS dissociators (Miltenyi®) or by mechanical disruption, followed by filtration
480 through a 70-µm nylon mesh. The cells were stained with anti-CD3 (AF700), anti-CD4 (APC),
481 anti-CD8 (FITC), and for some samples, anti-CD25 (PE) antibodies. Cell sorting was performed
482 by fluorescent activated cell sorting (FACS) on a Becton Dickinson FACSAriaII, achieving a
483 purity of >85%. The sorted populations included DP CD3+ (CD3+CD4+CD8+), SP CD8+
484 (CD3+CD4-CD8+), and SP CD4+ (CD3+CD4+CD8-). A further separation was made into SP CD4
485 Teff (CD3+CD4+CD8-CD25-) and SP CD4 Treg (CD3+CD4+CD8-CD25+) for sixteen of the
486 samples (**Figure 1**). For the sorted SP CD4, the Treg percentage varied between 5.8% and 16%
487 across samples, with an average of 9.63%. Six samples of SP CD4 samples were not sorted into

488 Teffs and Tregs, we thus categorized them as SP CD4 Teffs, assuming a purity of Teffs within
489 the total SP CD4 of around 90%. Please refer to the detailed sample metadata in
490 **Supplementary Table 3** of the supplementary material. This includes donor IDs and the
491 number of sorted cells per thymic subset for each donor.
492 The RNA was isolated using the RNAqueous extraction kit (Invitrogen®), in accordance with
493 the manufacturer's protocol. The RNA samples were quantified and the integrity of each
494 sample was determined using a Nanodrop (Thermo Fisher) or a Tapestation 4200 (Agilent,
495 RNA ScreenTape).

496 ***TCR library preparation and sequencing***

497 TCR library preparation and sequencing were performed as described by Barennes et al. (57).
498 Briefly, RNA was processed using the SMARTer Human TCR a/b profiling v1 kit (Takarabio), in
499 accordance with the manufacturer's protocol. Amplicons were then purified using AMPure
500 XP beads (Beckman Coulter) and their quantity was determined. The integrity of the
501 amplicons was then assessed using the 2100 Bioanalyzer System (Agilent, DNA 1000 kit) or
502 Tapestation 4200 (Agilent, D1000 screentape). Bulk Next-Generation Sequencing was
503 performed using either a Hiseq 2500 (Illumina) with the SR-300 protocol plus 10% PhiX on the
504 LIGAN-PM Genomics platform (Lille, France), or a Novaseq 6000 (Illumina) with the PE-250
505 protocol plus 10% PhiX on the LIGAN-PM Genomics platform or ICM platform (Paris, France).

506 ***Data processing***

507 The raw FASTQ/FASTA files were aligned to TRA and TRB using MiXCR (v3.0.13, RNA-seq
508 parameters), a software solution that is able to correct for both sequencing and PCR errors
509 (58). Samples with fewer than 1,000 CDR3aa sequences, an imbalanced TRA/TRB ratio (<1/9),
510 or a low sequence count relative to sorted cell counts (< 0.9 ratio) were removed. Sequences
511 with CDR3aa lengths outside 6-23 amino acids were also discarded. To standardize clonotype

512 counts and the number of unique clonotypes across sequencing techniques, the initial counts
513 for each clonotype were reduced by 1 to exclude those with counts of 0 (singletons).
514 Furthermore, due to the high similarity between certain TRBV sequences, which has the
515 potential to influence the analysis depending on the sequencing method used, TRBV06-2 and
516 TRBV06-3 were merged as TRBV06-2/3, and TRBV12-3 and TRBV12-4 were combined as
517 TRBV12-3/4 (59). Please refer to the summary table provided in the supplementary material
518 (**Supplementary Table 3**) for a comprehensive overview of the total number of TCR sequences
519 retained after preprocessing, as well as the corresponding number of unique clonotypes, for
520 each donor, chain and thymic subset.

521 ***Gene usage analysis***

522 For both TRA and TRB chains across all cell subtypes, we analyzed the V and J gene usage and
523 those of the VJ gene associations (**Figure 1**).

524 The usage of gene is calculated as follows: $\frac{\Sigma i \epsilon G^{ci}}{\Sigma j \epsilon S^{cj}}$

525 Where:

526 - $\Sigma i \epsilon G^{ci}$ represents the total number of counts for clonotypes associated with the
527 specified gene or gene association.
528 - $\Sigma j \epsilon S^{cj}$ represents the total sum of the counts of all clonotypes in the sample.

529 In this notation, G is the set of clonotypes using the interested gene, S is the set of all
530 clonotypes in the sample, and c_i and c_j are the counts of the clonotypes *i* and *j*, respectively.
531 The usage of the V gene and the VJ gene combinations was investigated through dimensional
532 reduction using Principal Component Analysis (PCA) (MASS package v7.3-60, factoMineR
533 package v2.8, factoextra package v1.0.7). Confidence ellipses were represented with a 5%
534 alpha risk. Furthermore, for VJ gene combinations usage, a heatmap was constructed using

535 the Jensen-Shannon Divergence (JSD) distance to measure the distance between samples
536 based on their gene usage distribution (complexHeatmap package v2.16.0, philentropy
537 package v0.7.0). Hierarchical clustering was performed using the Euclidean distance and the
538 complete linkage method.

539 ***Diversity analysis***

540 For the TCR repertoire diversity analysis, to correct for sequencing depth bias and differences
541 in cellular richness between individuals, rarefactions were performed fifty times for each
542 sample, using X clonotypes, where X represents the effective diversity number (60).
543 The effective diversity was calculated as the exponential of the Shannon index (e^H) (61).
544 Rényi indices (11 indices from 0 to Infinity) were calculated for each rarefaction (62).
545 The median Shannon index, Simpson index and Berger-Parker indices were then compared
546 between the sexes.

547 ***Distribution of CDR3aa length analysis***

548 The calculation of the usage of all CDR3 by the amino acid length as follows: $\frac{\Sigma i \epsilon L^{ci}}{\Sigma j \epsilon S^{cj}}$

549 Where

550 - $\Sigma i \epsilon L^{ci}$ represents the sum of the counts of the CDR3 characterized by the amino acid
551 length of interest.
552 - $\Sigma j \epsilon S^{cj}$ represents the total sum of counts of all CDR3s per sample.

553 In this notation, L is the set of CDR3s characterized by the amino acid length of interest, S is
554 the set of all CDR3s in the sample, and c_i and c_j are the counts of the CDR3s *i* and *j*, respectively.

555 ***Composition usage of amino acid within the CDR3 region***

556 All CDR3aa sequences were aligned using the IMGT convention (positions p104-p118) (63).

557 Three complementary scales were used in the study. Firstly, sequence level amino acid
558 composition. Within the CDR3 loop region (IMGT positions p108-p114), involved in MHC-
559 peptide complex interaction (63), amino acid usage at the sequence level was quantified for
560 CDR3aa sequences 9-21 aa long in both TRA and TRB chains. For each sequence, the
561 percentage usage of a given amino acid was calculated as follows:

562 (1) CDR3aa loop usage (%) = $\frac{n_{aa}}{L}$ x 100

563 Where n_{aa} is the number of occurrences of the amino acid of interest in the CDR3 loop, and
564 L denotes the total length of the CDR3aa sequence. Furthermore, amino acids were
565 categorized into three hydropathy classifications (neutral, hydrophobic, and hydrophilic)
566 using the IMGT classification that takes into account the Kyte-Doolittle hydropathy index
567 (25,64)

568 Secondly, the position-specific amino acid usage at p109 and p110. To assess positional
569 composition, for each individual, CDR3aa usage is examined at IMGT positions p109 and p110,
570 corresponding to p6-p7 positions described by Stadinsky et al. and Khosravi-Maharlooei et
571 al., which hydrophobic amino acids at these two central positions have been implicated in
572 modulating TCR self-reactivity and cross-reactivity (26–28). For a hydrophobic amino acid h
573 (excluding alanine, due to its weak hydrophobicity) at position p, usage was defined:

574 (2) Hydrophobic CDR3aa usage in position (%) = $\frac{N_{(h,p)}}{n}$ x 100

575 Where n is the total number of unique CDR3 sequences and $N_{(h,p)}$ the number of unique CDR3
576 sequences carrying hydrophobic amino acid a at position p. This analysis quantifies amino
577 acid composition at fixed positions independently of clonotype frequency.

578 ***Probability of generation analysis***

579 The probability of generation analysis of DP and CD8 cell subtypes consisted initially in the
580 creation of a generative model of V(D)J recombination using 400,000 randomly selected non-

581 productive sequences from all samples for both TRA and TRB chains, with the IGOR tool (65).
582 The generation probabilities (Pgen) for all sequences in the dataset were subsequently
583 calculated using the OLGA tool, based on the respective generative models for each cell
584 subtype and TCR chain (66). Comparisons of Pgen values at the nucleotide level between
585 males and females were performed. To ensure statistical robustness, control groups with
586 equivalent male and female sample numbers were created by permuting the samples into
587 two groups 20,000 times.

588 ***TCR network structure by sequence similarity***

589 For each sample, 100 random sub-samplings of CDR3aa sequences were performed, using the
590 minimum CDR3aa count per cell subtype (refer to **Supplementary Table 1**). Two CDR3aa were
591 connected if their Levenshtein distance was = 1 (**Figure 1**) (67). Network analysis focused on
592 two metrics: the proportion of connected sequences and network density, defined as the
593 ratio of actual connections to all possible connections. Median values from 100 subsampling
594 iterations were then analyzed. Levenshtein distances were computed with the stringdist
595 package (v0.9.10), networks were visualized using Cytoscape (v3.8.2), and network density
596 was calculated with the igraph package (v1.5.1).

597 ***TRB CDR3aa motif search***

598 Two types of structural motifs were searched: local motifs (strict sequential motifs) and global
599 motifs (sequences with substitutions preserving a positive BLOSUM62 score) (Figure 1).
600 The selection of enriched motifs was carried out using the gliph2 function with the turboGliph
601 package (v0.99.2), with specific parameters defined as follows:

602 - The input sequences were from the sex group of interest (male or female), with
603 reference sequences matched for TRBV gene usage.
604 - It is imperative that CDR3aa sequences are longer than eight aa.

605 - Local motif lengths were restricted to 3-5 aa.

606 - Only motifs consisting of more than two unique CDR3aa were conserved.

607 - Local motif significance of Fisher's test has not been boosted.

608 Additional filters were applied so that: (i) the inclusion of public CDR3aa sequences is a
609 prerequisite for a motif, with these sequences shared by at least two individuals, (ii) a
610 significant enrichment is required, as determined by Fisher's test with a p-value $p < 0.01$ and
611 (iii) a usage difference between groups of at least twofold is necessary, as evidenced by a
612 Wilcoxon test with a p-value $p < 0.05$.

613 Motif validation was performed on an openly published pediatric thymic dataset from the
614 Arstila team (35,36) consisting in a bulk TCR dataset from infants aged between seven days
615 and eight months. Here, we removed one male subject, "Thymus A", who was a twin of the
616 "Thymus B" and "Thymus 1" neonate sample, in order to analyze height samples with a male-
617 to-female ratio of 5:3. Further validation was conducted on sorted peripheral blood TCR
618 repertoires (CD8, CD4 Teff and CD4 Treg) from seventy-five healthy volunteers aged from
619 eighteen to eighty-four years (male-to-female ratio of 1.03:1), whose libraries were
620 generated under the same conditions as those of our thymic dataset. They were recruited
621 within the Transimmunom observational trial (NCT02466217) and HEALTHIL-2
622 (NCT03837093) (68). PBMCs from healthy individuals were isolated using Ficoll density
623 gradient centrifugation and enriched for CD4+ T cells via EasySep™ Human CD4+ T Cell
624 magnetic beads (Stemcell). The samples were then separated into two groups: effector T cells
625 (CD4+ CD25-) and Tregs (CD4+ CD25+). This was done using EasySep™ Human Pan-CD25
626 magnetic beads (Stemcell). Purity was assessed by flow cytometry based on the expression of
627 CD4 and FoxP3, with a purity threshold of >80%. From the frozen PBMC aliquots, CD8+ T cells
628 (CD3+ CD8+) were sorted using a FACS ARIA II cell sorter.

629 ***TRB CDR3aa specificity analysis***

630 We have established a curated and harmonized TCR specificity database by integrating data
631 from three public TCR repositories: Mc-PAS, IEDB, and VDJdb (38,39,69) (data collected as of
632 October 2023) (**Figure 1**). The harmonization procedure was carried out in accordance with
633 the framework outlined in Jouannet et al. (70) and included :

634 - Uniform formatting of TRA/TRB TCR sequences and associated metadata,
635 - Consolidation of redundant entries (identical TRA/TRB TCR, epitope, organism,
636 PubMed ID, and cell subset),
637 - Maintening separate entries when source databases are incompatible,

638 Reliability levels for sequences and specificity assignments were quantified using the
639 Verified_score (VS) and Antigen-identification_score (AIS) as defined in (70). The VS, ranging
640 from 0 to 2, reflects the concordance between calculated and curated CDR3 boundaries
641 following the IEDB verification strategy (VS = 2: both TRA and TRB present and verified; VS =
642 1.1: only TRA verified; VS = 1.2: only TRB verified; VS = 0: no verified chain) and the AIS (0 to
643 5), which ranks the strength of antigen-identification methods (70).

644 In this study, we focused our analyses on high-reliability TRB sequences, defined as those with
645 a verified TRB CDR3aa (VS ≥ 1.2) and an AIS corresponding to in vitro T cell stimulation with a
646 pathogen, protein or peptide, or pMHC X-mer sorting (AIS > 3.2, excluding categories 4.1 and
647 4.2). This ensures that the specificity assignments relied on robust experimental evidence.

648 Specificity groups were categorized according to antigen class, encompassing viral, bacterial,
649 yeast, parasitic and self-antigens along with antigens derived from wheat, plants or animals.
650 Self-antigens were then annotated into three categories: autoimmune-associated antigens,
651 cancer-associated antigens and self-antigens unrelated to disease. For autoimmune-
652 associated antigens, assignments were based on explicit annotations present in McPAS-TCR,

653 IEDB and VDJdb. These databases identify celiac disease (CeD) and type 1 diabetes (T1D)
654 related antigens, which were retained as such in the harmonized dataset. For cancer-
655 associated antigens, the following classifications were used: (i) information present in the
656 original databases and (ii) cross-referencing with external cancer antigen resources, including
657 the Cancer Antigenic Peptide Database (de Duve Institute), the Human Protein Atlas and the
658 cancer database caAtlas (71). Please refer to **Supplementary Table 4**, which provides a
659 comprehensive list of all self-antigens present in the harmonized database. This table also
660 includes their associated disease category and their mapping into the specificity groups used
661 in the manuscript.
662 This harmonized database was used to identify exact matches with the CDR3aa sequences of
663 our TRB sequences. The enrichment of CDR3aa sequences associated with a given specificity
664 group in male and female thymic repertoires for each cell subtype compared to the specificity
665 distribution in the database was tested. Furthermore, we performed specificity group
666 distributions between male and female samples, as well as was the overall usage of these
667 sequences across entire TCR repertoires.
668 Additionally, our research concentrated on polyspecific sequences defined as CDR3aa TRB
669 sequences recognizing at least two distinct microbial species or belonging to multiple
670 specificity groups for non-microbial antigens. In this study, polyspecificity is therefore
671 considered at the level of broader antigenic categories rather than individual epitopes and
672 thus reflects functional cross-reactivity patterns aggregated across studies, instead of
673 implying molecular-level multi-epitope recognition. These polyspecific TRB CDR3aa
674 sequences underwent the same statistical analyses as monofunctional sequences.

675 ***Statistical analysis***

676 For V-J gene usage, CDR3aa length usage, CDR3aa usage, network similarity and specificity
677 analyses, the comparison between males and females was statistically analysed using the
678 Wilcoxon test. The statistical tests were performed using the ggpubr library (v0.6.0) in R. The
679 number of asterisks denotes the significance of the results: one asterisk indicates a p-value p
680 ≤ 0.05, two asterisk indicate a p-value p ≤ 0.01, and so on until four asterisks, denoting a p-
681 value p ≤ 0.0001. The comparisons of the Rényi curves and Pgen were compared using the
682 Kolmogorov-Smirnov test. The Wilcoxon test was used to test the comparisons of the
683 proportions of specific sequences in male and female subjects relative to those in the
684 specificity database.

685 ***Data availability***

686 All raw sequencing data generated in this study are publicly available on NCBI under the
687 BioProject accession PRJNA1379632 (https://www.ncbi.nlm.nih.gov/sra/PRJNA1379632).

688 Author contributions

689 VQ and HV conducted all cell sorting. RNA extraction and TCR library preparation were
690 performed by HV, VQ, LA, PB, NC, VD, JD, GF, KL and PS. HV, VQ, VM, LA, KL, ONT, MP, PS, AS,
691 EMF and DK contributed valuable suggestions for experimental design and participated in
692 discussions of the results. HV and CJ pooled and curated the reference specificity database.
693 LA, CJ and VM contributed equally in this work. HV authored the manuscript, with VQ, VM,
694 CA, JD, EMF and DK providing comments and critical reviews. DK conceptualized, supervised
695 and provided funding for the study.

Acknowledgment

We would like to thank Bruno Gouritin for his assistance with cell sorting and to Marie Surroque for her support with RNA quantification.

During manuscript preparation, the authors used ChatGPT (OpenAI) solely to assist with language editing (syntax, grammar and phrasing). All ideas, analyses, interpretations and scientific reasoning are the authors' own.

Funding Statement

This work was supported by the TRiPoD European Research Council-Advanced EU (No. 322856), the LabEx Transimmunom (ANR-11-IDEX-0004-02) and the iMAP (ANR-16-RHUS-0001) grants to DK and the iReceptorPlus (Horizon 2020 No. 825821) and additional support from Sorbonne Université, INSERM as well as Intitut Universitaire de France. KLG was supported by the European Research Area Network-Cardiovascular Diseases [ERANET-CVD JCT2018, AIR-MI Consortium (ANR-18-ECVD-0001)] grant to EMF.

References

1. Libert C, Dejager L, Pinheiro I. The X chromosome in immune functions: when a chromosome makes the difference. Nat Rev Immunol. 2010 Aug;10(8):594–604.

2. Golden LC, Voskuhl R. The Importance of Studying Sex Differences in Disease: The Example of Multiple Sclerosis. J Neurosci Res. 2017 Jan 2;95(1–2):633–43.

3. Sokka T, Toloza S, Cutolo M, Kautiainen H, Makinen H, Gogus F, et al. Women, men, and rheumatoid arthritis: analyses of disease activity, disease characteristics, and treatments in the QUEST-RA Study. Arthritis Res Ther. 2009;11(1):R7.

4. Li Y, Jerkic M, Slutsky AS, Zhang H. Molecular mechanisms of sex bias differences in COVID-19 mortality. Crit Care. 2020 July 9;24:405.

5. Hertz D, Schneider B. Sex differences in tuberculosis. Semin Immunopathol. 2019 Mar 1;41(2):225–37.

6. Klein SL, Morgan R. The impact of sex and gender on immunotherapy outcomes. Biol Sex Differ. 2020 May 4;11(1):24.

7. Lee HJ, Chang C. Recent advances in androgen receptor action. Cell Mol Life Sci CMLS. 2003 Aug 1;60(8):1613–22.

8. Chen P, Li B, Ou-Yang L. Role of estrogen receptors in health and disease. Front Endocrinol. 2022 Aug 18;13:839005.

9. Scarpin KM, Graham JD, Mote PA, Clarke CL. Progesterone action in human tissues: regulation by progesterone receptor (PR) isoform expression, nuclear positioning and coregulator expression. Nucl Recept Signal. 2009 Dec 31;7:e009.

10. Klein L, Kyewski B, Allen PM, Hogquist KA. Positive and negative selection of the T cell repertoire: what thymocytes see (and don't see). Nat Rev Immunol. 2014 June;14(6):377–91.

11. Zhu ML, Bakhru P, Conley B, Nelson JS, Free M, Martin A, et al. Sex bias in CNS autoimmune disease mediated by androgen control of autoimmune regulator. Nat Commun. 2016 Apr 13;7(1):11350.

12. Dragin N, Bismuth J, Cizeron-Clairac G, Biferi MG, Berthault C, Serraf A, et al. Estrogen-mediated downregulation of AIRE influences sexual dimorphism in autoimmune diseases. J Clin Invest. 126(4):1525–37.

13. Stankiewicz LN, Salim K, Flaschner EA, Wang YX, Edgar JM, Durland LJ, et al. Sex-biased human thymic architecture guides T cell development through spatially defined niches. Dev Cell. 2024 Oct 3;S1534-5807(24)00539-2.

14. Murugan A, Mora T, Walczak AM, Callan CG. Statistical inference of the generation probability of T-cell receptors from sequence repertoires. Proc Natl Acad Sci. 2012 Oct 2;109(40):16161–6.

15. Yoshida K, Cologne JB, Cordova K, Misumi M, Yamaoka M, Kyoizumi S, et al. Aging-related changes in human T-cell repertoire over 20 years delineated by deep sequencing of peripheral T-cell receptors. Exp Gerontol. 2017 Oct 1;96:29–37.

16. Trofimov A, Brouillard P, Larouche JD, Séguin J, Laverdure JP, Brasey A, et al. Two types of human TCR differentially regulate reactivity to self and non-self antigens. iScience. 2022 Aug 17;25(9):104968.

17. Mika J, Yoshida K, Kusunoki Y, Candéias SM, Polanska J. Sex- and age-specific aspects of human peripheral T-cell dynamics. Front Immunol. 2023 Oct 13;14:1224304.

18. Gong M, Li X, Zheng A, Xu H, Xie S, Yan R, et al. Age-related changes in the TRB and IGH repertoires in healthy adult males and females. Immunol Lett. 2021 Dec 1;240:71–6.

19. Qi Q, Liu Y, Cheng Y, Glanville J, Zhang D, Lee JY, et al. Diversity and clonal selection in the human T-cell repertoire. Proc Natl Acad Sci U S A. 2014 Sept 9;111(36):13139–44.

20. Davis MM, Bjorkman PJ. T-cell antigen receptor genes and T-cell recognition. Nature. 1988 Aug;334(6181):395–402.

21. Wang F, Ono T, Kalergis AM, Zhang W, DiLorenzo TP, Lim K, et al. On defining the rules for interactions between the T cell receptor and its ligand: a critical role for a specific amino acid residue of the T cell receptor beta chain. Proc Natl Acad Sci U S A. 1998 Apr 28;95(9):5217–22.

765 22. Yu K, Shi J, Lu D, Yang Q. Comparative analysis of CDR3 regions in paired human αβ
766 CD8 T cells. FEBS Open Bio. 2019 July 12;9(8):1450–9.

767 23. Carter JA, Preall JB, Grigaityte K, Goldfless SJ, Jeffery E, Briggs AW, et al. Single T
768 Cell Sequencing Demonstrates the Functional Role of αβ TCR Pairing in Cell Lineage
769 and Antigen Specificity. Front Immunol. 2019;10:1516.

770 24. Garcia KC, Degano M, Pease LR, Huang M, Peterson PA, Teyton L, et al. Structural
771 basis of plasticity in T cell receptor recognition of a self peptide-MHC antigen. Science.
772 1998 Feb 20;279(5354):1166–72.

773 25. Pommié C, Levadoux S, Sabatier R, Lefranc G, Lefranc MP. IMGT standardized criteria
774 for statistical analysis of immunoglobulin V-REGION amino acid properties. J Mol
775 Recognit. 2004;17(1):17–32.

776 26. Khosravi-Maharlooei M, Obradovic A, Misra A, Motwani K, Holzl M, Seay HR, et al.
777 Crossreactive public TCR sequences undergo positive selection in the human thymic
778 repertoire. J Clin Invest. 2019 Mar 28;129(6):2446–62.

779 27. Lu J, Van Laethem F, Bhattacharya A, Craveiro M, Saba I, Chu J, et al. Molecular
780 constraints on CDR3 for thymic selection of MHC-restricted TCRs from a random pre-
781 selection repertoire. Nat Commun. 2019 Mar 4;10:1019.

782 28. Stadinski BD, Shekhar K, Gómez-Touriño I, Jung J, Sasaki K, Sewell AK, et al.
783 Hydrophobic CDR3 residues promote the development of self-reactive T cells. Nat
784 Immunol. 2016 Aug;17(8):946–55.

785 29. Elhanati Y, Murugan A, Callan CG, Mora T, Walczak AM. Quantifying selection in
786 immune receptor repertoires. Proc Natl Acad Sci U S A. 2014 July 8;111(27):9875–80.

787 30. Meysman P, De Neuter N, Gielis S, Bui Thi D, Ogunjimi B, Laukens K. On the viability
788 of unsupervised T-cell receptor sequence clustering for epitope preference.
789 Bioinformatics. 2019 May 1;35(9):1461–8.

790 31. Springer I, Tickotsky N, Louzoun Y. Contribution of T Cell Receptor Alpha and Beta
791 CDR3, MHC Typing, V and J Genes to Peptide Binding Prediction. Front Immunol. 2021
792 Apr 26;12:664514.

793 32. Korpela D, Jokinen E, Dumitrescu A, Huuhtanen J, Mustjoki S, Lähdesmäki H. EPIC-
794 TRACE: predicting TCR binding to unseen epitopes using attention and contextualized
795 embeddings. Bioinformatics. 2023 Dec 9;39(12):btad743.

796 33. Huang H, Wang C, Rubelt F, Scriba TJ, Davis MM. Analyzing the Mycobacterium
797 tuberculosis immune response by T-cell receptor clustering with GLIPH2 and genome-
798 wide antigen screening. Nat Biotechnol. 2020 Oct;38(10):1194–202.

799 34. Henikoff S, Henikoff JG. Amino acid substitution matrices from protein blocks. Proc
800 Natl Acad Sci U S A. 1992 Nov 15;89(22):10915–9.

801 35. Heikkilä N, Kleino I, Vanhanen R, Yohannes DA, Mattila IP, Saramäki J, et al.
802 Characterization of human T cell receptor repertoire data in eight thymus samples and
803 four related blood samples. Data Brief. 2021 Apr 1;35:106751.

36. Mattila J, Sormunen S, Heikkilä N, Mattila IP, Saramäki J, Arstila TP. Analysis of thymic generation of shared T-cell receptor α repertoire associated with recognition of tumor antigens shows no preference for neoantigens over wild-type antigens. Cancer Med. 2023 June;12(12):13486–96.

37. Vita R, Mahajan S, Overton JA, Dhanda SK, Martini S, Cantrell JR, et al. The Immune Epitope Database (IEDB): 2018 update. Nucleic Acids Res. 2018 Oct 24;47(Database issue):D339.

38. Tickotsky N, Sagiv T, Prilusky J, Shifrut E, Friedman N. McPAS-TCR: a manually curated catalogue of pathology-associated T cell receptor sequences. Bioinforma Oxf Engl. 2017 Sept 15;33(18):2924–9.

39. Shugay M, Bagaev DV, Zvyagin IV, Vroomans RM, Crawford JC, Dolton G, et al. VDJdb: a curated database of T-cell receptor sequences with known antigen specificity. Nucleic Acids Res. 2018 Jan 4;46(D1):D419–27.

40. Rosati E, Dowds CM, Liaskou E, Henriksen EKK, Karlsen TH, Franke A. Overview of methodologies for T-cell receptor repertoire analysis. BMC Biotechnol. 2017 July 10;17(1):61.

41. Wooldridge L, Ekeruche-Makinde J, van den Berg HA, Skowera A, Miles JJ, Tan MP, et al. A single autoimmune T cell receptor recognizes more than a million different peptides. J Biol Chem. 2012 Jan 6;287(2):1168–77.

42. Hadrup SR, Bakker AH, Shu CJ, Andersen RS, van Veluw J, Hombrink P, et al. Parallel detection of antigen-specific T-cell responses by multidimensional encoding of MHC multimers. Nat Methods. 2009 July;6(7):520–6.

43. Quiniou V, Barennes P, Mhanna V, Stys P, Vantomme H, Zhou Z, et al. Human thymopoiesis produces polyspecific CD8+ α/β T cells responding to multiple viral antigens. eLife. 2023 Mar 30;12:e81274.

44. van de Sandt CE, Nguyen THO, Gherardin NA, Crawford JC, Samir J, Minervina AA, et al. Newborn and child-like molecular signatures in older adults stem from TCR shifts across human lifespan. Nat Immunol. 2023 Nov;24(11):1890–907.

45. Schneider-Hohendorf T, Görlich D, Savola P, Kelkka T, Mustjoki S, Gross CC, et al. Sex bias in MHC I-associated shaping of the adaptive immune system. Proc Natl Acad Sci U S A. 2018 Feb 27;115(9):2168–73.

46. Roca AM, Chobrutskiy BI, Callahan BM, Blanck G. T-cell receptor V and J usage paired with specific HLA alleles associates with distinct cervical cancer survival rates. Hum Immunol. 2019 Apr;80(4):237–42.

47. Hou X, Wei W, Zhang J, Liu Z, Wang G, Yang X, et al. Characterisation of T and B cell receptor repertoire in patients with systemic lupus erythematosus. Clin Exp Rheumatol. 2023 Nov;41(11):2216–23.

48. Rojas M, Restrepo-Jiménez P, Monsalve DM, Pacheco Y, Acosta-Ampudia Y, Ramírez-Santana C, et al. Molecular mimicry and autoimmunity. J Autoimmun. 2018 Dec 1;95:100–23.

844 49. Repac J, Božić B, Božić Nedeljković B. Microbes as triggers and boosters of Type 1
845 Diabetes - Mediation by molecular mimicry. Diabetes Res Clin Pract. 2023
846 Aug;202:110824.

847 50. Girdhar K, Huang Q, Chow IT, Vatanen T, Brady C, Raisingani A, et al. A gut microbial
848 peptide and molecular mimicry in the pathogenesis of type 1 diabetes. Proc Natl Acad Sci
849 U S A. 2022 Aug 2;119(31):e2120028119.

850 51. Petersen J, Ciacchi L, Tran MT, Loh KL, Kooy-Winkelaar Y, Croft NP, et al. T cell
851 receptor cross-reactivity between gliadin and bacterial peptides in celiac disease. Nat
852 Struct Mol Biol. 2020 Jan;27(1):49–61.

853 52. Vazquez DS, Schilbert HM, Dodero VI. Molecular and Structural Parallels between
854 Gluten Pathogenic Peptides and Bacterial-Derived Proteins by Bioinformatics Analysis.
855 Int J Mol Sci. 2021 Aug 27;22(17):9278.

856 53. Tai N, Peng J, Liu F, Gulden E, Hu Y, Zhang X, et al. Microbial antigen mimics activate
857 diabetogenic CD8 T cells in NOD mice. J Exp Med. 2016 Sept 19;213(10):2129–46.

858 54. Hebbandi Nanjundappa R, Sokke Umeshappa C, Geuking MB. The impact of the gut
859 microbiota on T cell ontogeny in the thymus. Cell Mol Life Sci. 2022 Apr;79(4):221.

860 55. Markle JGM, Frank DN, Mortin-Toth S, Robertson CE, Feazel LM, Rolle-Kampczyk U,
861 et al. Sex differences in the gut microbiome drive hormone-dependent regulation of
862 autoimmunity. Science. 2013 Mar 1;339(6123):1084–8.

863 56. Ghoreyshi Z, George J. Quantitative approaches for decoding the specificity of the
864 human T cell repertoire. Front Immunol. 2023 Sept 7;14.

865 57. Barennes P, Quiniou V, Shugay M, Egorov ES, Davydov AN, Chudakov DM, et al.
866 Benchmarking of T cell receptor repertoire profiling methods reveals large systematic
867 biases. Nat Biotechnol. 2021 Feb;39(2):236–45.

868 58. Bolotin DA, Poslavsky S, Mitrophanov I, Shugay M, Mamedov IZ, Putintseva EV, et al.
869 MiXCR: software for comprehensive adaptive immunity profiling. Nat Methods. 2015
870 May;12(5):380–1.

871 59. Omer A, Peres A, Rodriguez OL, Watson CT, Lees W, Polak P, et al. T cell receptor beta
872 germline variability is revealed by inference from repertoire data. Genome Med. 2022 Jan
873 7;14(1):2.

874 60. Chaara W, Gonzalez-Tort A, Florez LM, Klatzmann D, Mariotti-Ferrandiz E, Six A.
875 RepSeq Data Representativeness and Robustness Assessment by Shannon Entropy. Front
876 Immunol. 2018 May 15;9:1038.

877 61. Shannon CE. The mathematical theory of communication. 1963. MD Comput Comput
878 Med Pract. 1997;14(4):306–17.

879 62. Rényi A. On Measures of Entropy and Information. In: Proceedings of the Fourth
880 Berkeley Symposium on Mathematical Statistics and Probability, Volume 1:
881 Contributions to the Theory of Statistics. University of California Press; 1961. p. 547–62.

882 63. Lefranc MP, Pommié C, Ruiz M, Giudicelli V, Foulquier E, Truong L, et al. IMGT
883 unique numbering for immunoglobulin and T cell receptor variable domains and Ig
884 superfamily V-like domains. Dev Comp Immunol. 2003 Jan;27(1):55–77.

885 64. Kyte J, Doolittle RF. A simple method for displaying the hydropathic character of a
886 protein. J Mol Biol. 1982 May 5;157(1):105–32.

887 65. Marcou Q, Mora T, Walczak AM. High-throughput immune repertoire analysis with
888 IGoR. Nat Commun. 2018 Feb 8;9(1):561.

889 66. Sethna Z, Elhanati Y, Callan CG, Walczak AM, Mora T. OLGA: fast computation of
890 generation probabilities of B- and T-cell receptor amino acid sequences and motifs.
891 Bioinforma Oxf Engl. 2019 Sept 1;35(17):2974–81.

892 67. Madi A, Poran A, Shifrut E, Reich-Zeliger S, Greenstein E, Zaretsky I, et al. T cell
893 receptor repertoires of mice and humans are clustered in similarity networks around
894 conserved public CDR3 sequences. eLife. 2017 July 21;6:e22057.

895 68. Lorenzon R, Mariotti-Ferrandiz E, Aheng C, Ribet C, Toumi F, Pitoiset F, et al. Clinical
896 and multi-omics cross-phenotyping of patients with autoimmune and autoinflammatory
897 diseases: the observational TRANSIMMUNOM protocol. BMJ Open. 2018 Aug
898 30;8(8):e021037.

899 69. Vita R, Mahajan S, Overton JA, Dhanda SK, Martini S, Cantrell JR, et al. The Immune
900 Epitope Database (IEDB): 2018 update. Nucleic Acids Res. 2019 Jan 8;47(D1):D339–43.

901 70. Jouannet C, Vantomme H, Gouge KL, Klatzmann D, Mariotti-Ferrandiz E.
902 Benchmarking unsupervised methods for inferring TCR specificity. NAR Genomics
903 Bioinforma. 2025 Dec 1;7(4):lqaf150.

904 71. Yi X, Liao Y, Wen B, Li K, Dou Y, Savage SR, et al. caAtlas: An immunopeptidome
905 atlas of human cancer. iScience. 2021 Oct 22;24(10):103107.

906

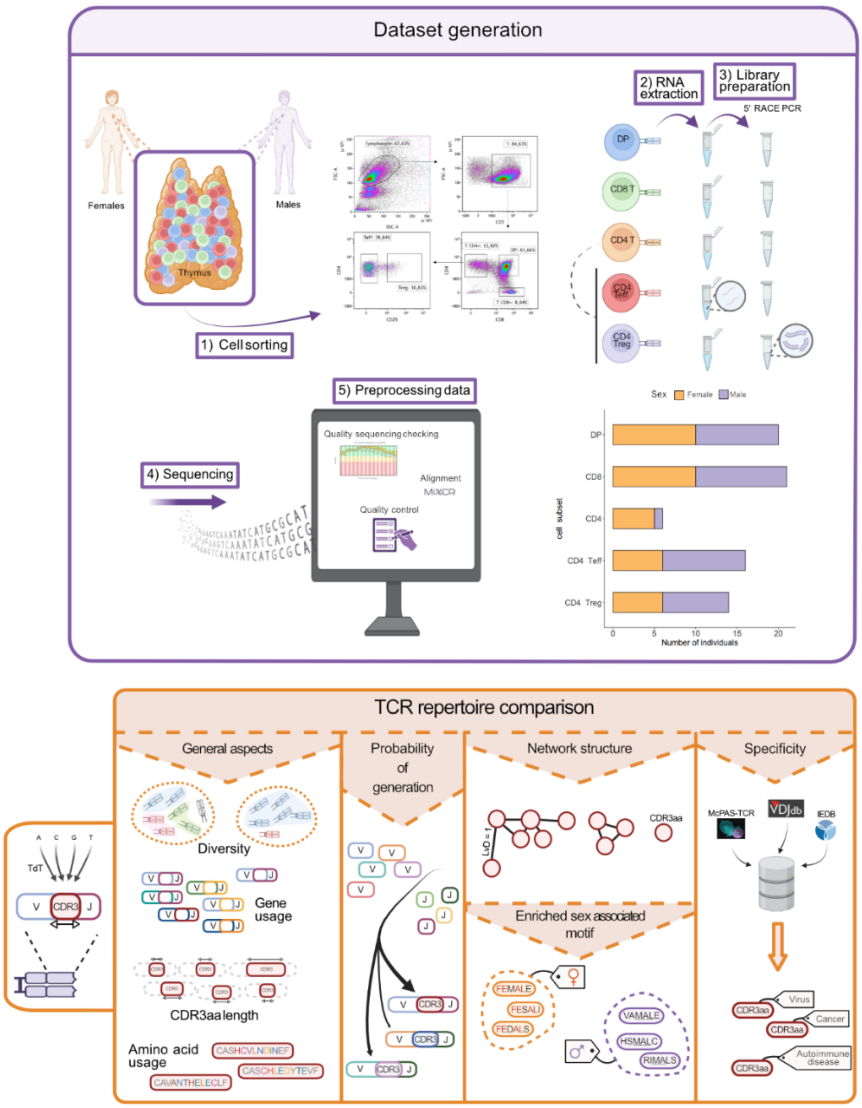

Figure 1: Schematic overview of the generation of the thymic TCR dataset and the analytical pipeline. Partially created with Biorender.com

Top Panel: Generation of the thymic TCR dataset. From deceased human thymuses of males and females, we isolated key T-cell subtypes through cell sorting. These subtypes included double-positive (DP) cells (CD3+ CD4+ CD8+), single-positive (SP) CD8+ cells (CD3+ CD4- CD8+), SP CD4+ cells (CD3+ CD4+ CD8-) that were further separated into T effector (Teff, CD3+ CD4+ CD8- CD25-) and Treg (CD3+ CD4+ CD8- CD25+) cells. TCR libraries were generated from the RNA of each cell population using rapid amplification of cDNA ends by PCR (5'RACE PCR). Following sequencing, data preprocessing involved quality sequencing checks, contig alignment, and quality control. The final dataset comprised 20 DP samples (male-to-female ratio of 1:1), 21 SP CD8+ samples (1.1:1), 6 SP CD4+ samples (1:5), 16 SP CD4 Teff samples (1.67:1), and 14 SP CD4 Treg samples (1.33:1). Males are depicted in violet and females in orange.

Bottom Panel: Analytical pipeline. We compared the TCR repertoires of males and females across various dimensions. We evaluated general aspects of the TCR repertoire were evaluated, including diversity, gene usage, CDR3aa length distribution, and aa usage within the CDR3 region. Additionally, we analyzed the probability of sequence generation and the TCR repertoire structure based on CDR3aa sequence similarity. We identified differentially expressed TRB CDR3aa motifs between sexes and analyzed TRB CDR3aa sequence specificity.

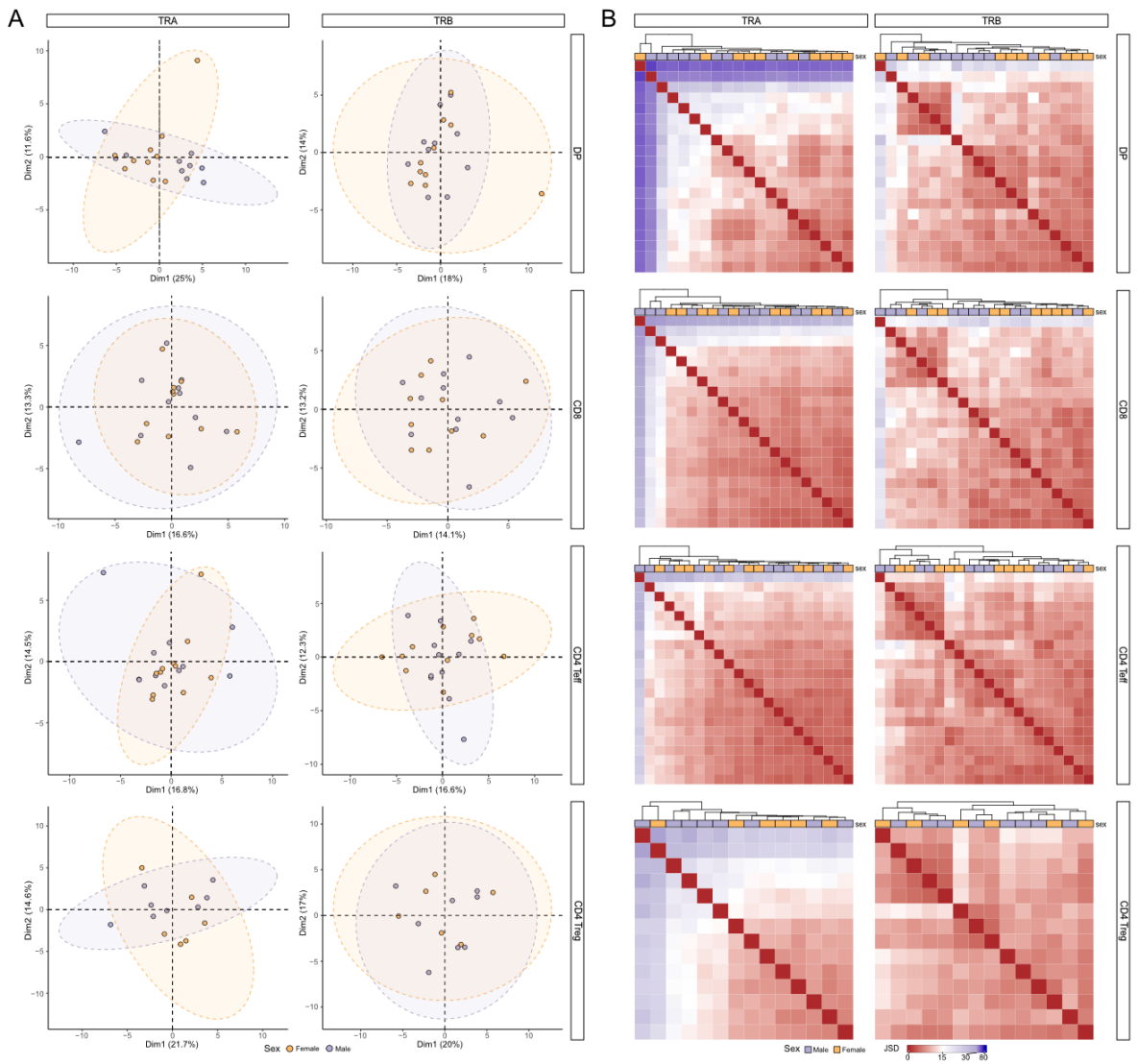

Figure 2: Comparable overall TCR gene usage between males and females.

(A) Principal Component Analysis (PCA) derived from the distribution of TRAV (left) and TRBV (right) gene usage frequencies across sex groups (males vs females), showing results for DP (N = 22), CD8 (N = 23), CD4 Teff (N = 24) and CD4 Treg (N = 14) cells (displayed from top to bottom). Each point on the graph represents an individual. Ellipses indicate 95% confidence intervals. **(B)** Heatmap showing the Jensen-Shannon Divergence (JSD) score between samples, derived from the distributional usage of TRAV-TRAJ (left) and TRBV-TRBJ (right) gene associations in DP (N = 22), CD8 (N = 23), CD4 Teff (N = 24) and CD4 Treg (N = 14) cells (displayed from top to bottom). Hierarchical clustering was performed using the Euclidean distance and the complete linkage method. Males are shown in violet; females in orange.

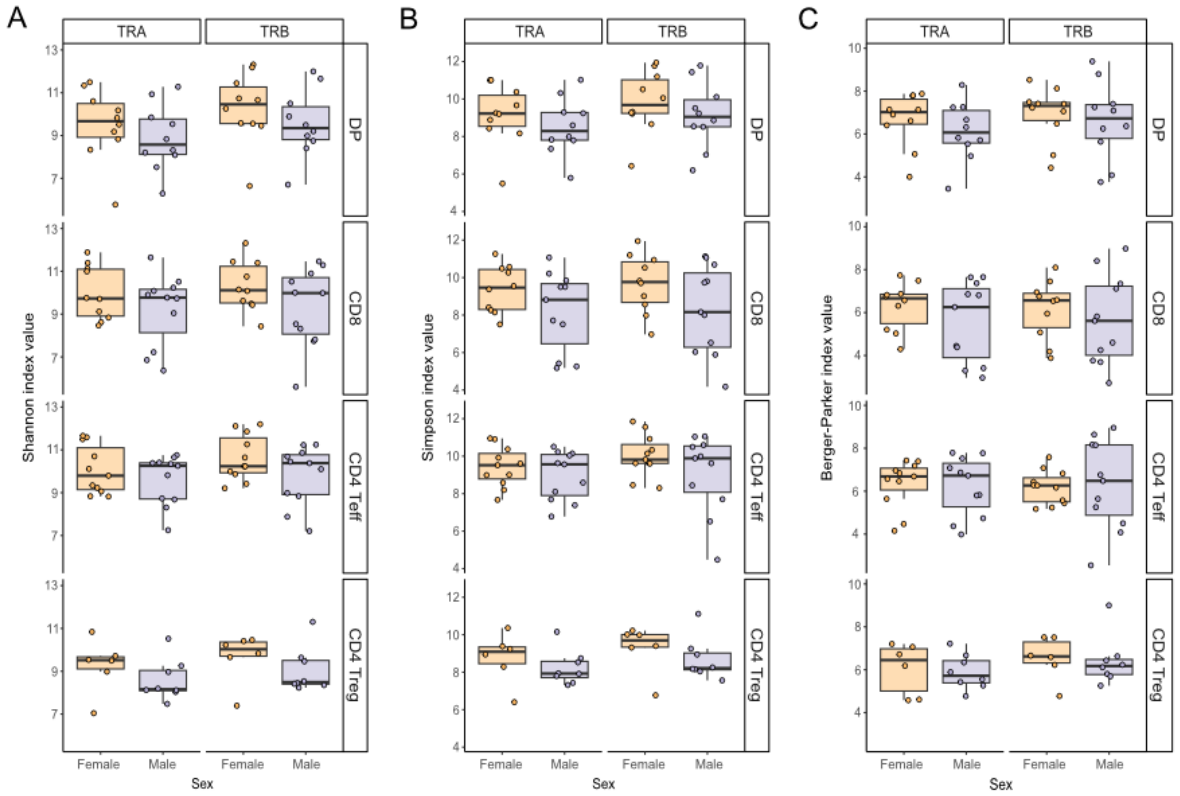

Figure 3: Comparable thymic TCR repertoire diversity between males and females.

Boxplots display Shannon **(A)**, Simpson **(B)**, and Berger-Parker **(C)** index values for TRA (left) and TRB (right), across thymic T cell subtypes, displayed from top to bottom, in DP (N = 22), CD8 (N = 23), CD4 Teff (N = 24) and CD4 Treg (N = 14). Each point on the graph represents the median value from 50 rarefactions per sample. Statistical analysis (Wilcoxon test) showed no significant sex bias in TCR repertoire diversity ($p > 0.05$). Males are shown in violet; females in orange.

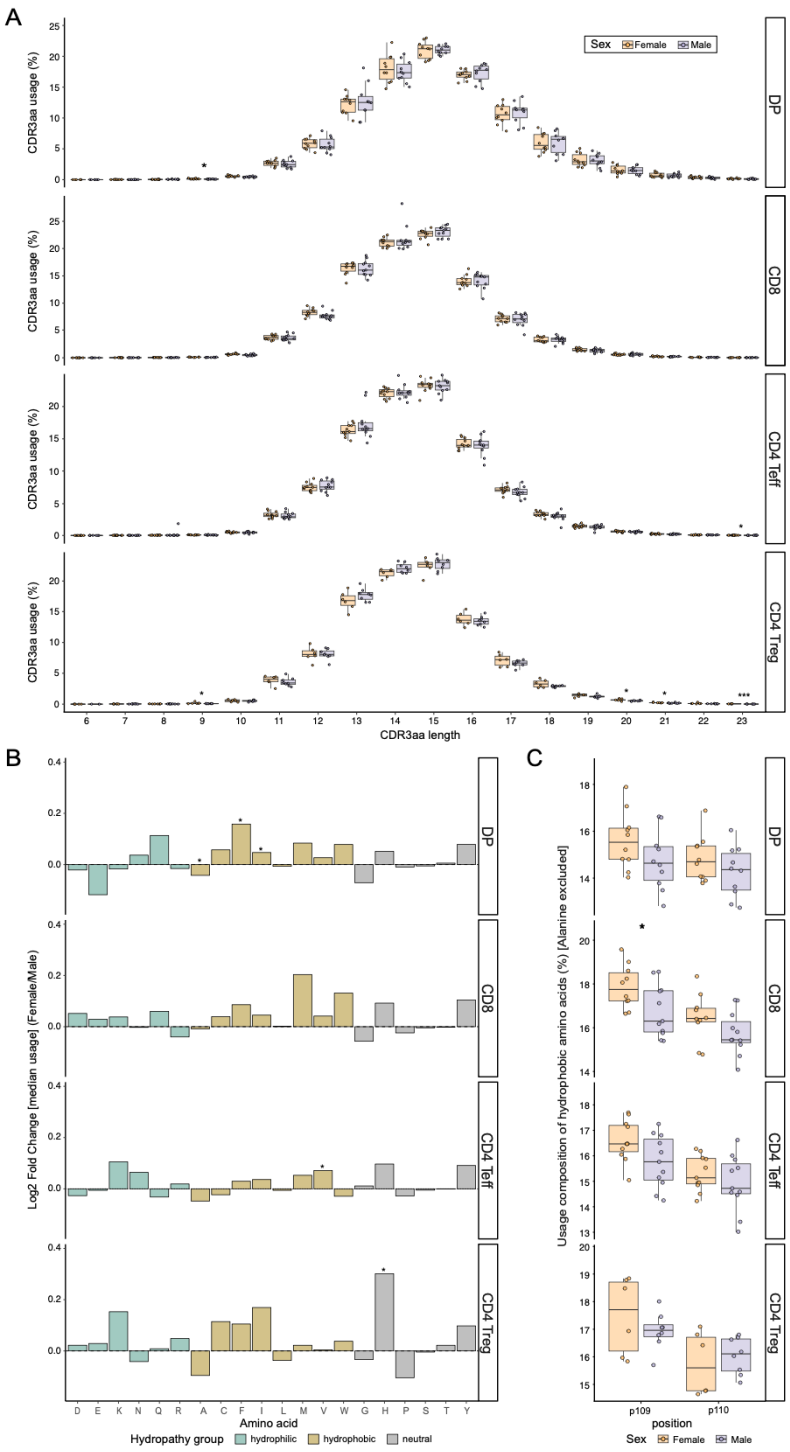

Figure 4: CDR3aa length and amino acid composition of TRB CDR3s in males and females.
(A) Distribution of TRB CDR3aa length usage in DP (N = 22), CD8 (N = 23), CD4 Teff (N = 24) and Treg (N = 14) SP cells (displayed from top to bottom). Stars indicate statistical differences between males and females based on the p-value of the Wilcoxon test (*: $p < 0.05$, **: $p < 0.01$). **(B)** The data on amino acid (aa) usage between males and females is presented as the log2 fold change of the median per-donor usage in females over males for each aa in the p108 to p114 CDR3aa region for TRB. A line at log2 fold change = 0 is indicative of the direction of the difference in usage frequency. The bars are colour-coded to the hydropathy class of the aa as defined by the Kyte-Doolittle-based IMGT classification (neutral aa by gray, hydrophilic aa by blue-green and hydrophobic aa by gold). Stars indicate statistical differences of usage between males and females based on the p-value of the Wilcoxon test (*: $p < 0.05$, **: $p < 0.01$). **(C)** Position-specific usage of hydrophobic aa (excluding alanine, due to its weak hydrophobicity) at IMGT positions p109 and p110 in TRB across thymic T cell subtypes, including DP (N = 22), CD8 (N = 23), CD4 Teff (N = 24) and CD4 Treg (N = 14). For each donor, the values represent the proportion of unique TRB CDR3aa sequences carrying a hydrophobic amino acid at the indicated position. Stars indicate significant sex differences based on the p-value of the Wilcoxon test (*: $p < 0.05$), with a significant increase in hydrophobic usage at p109 in female CD8 SP cells. Males are depicted in violet; females in orange.

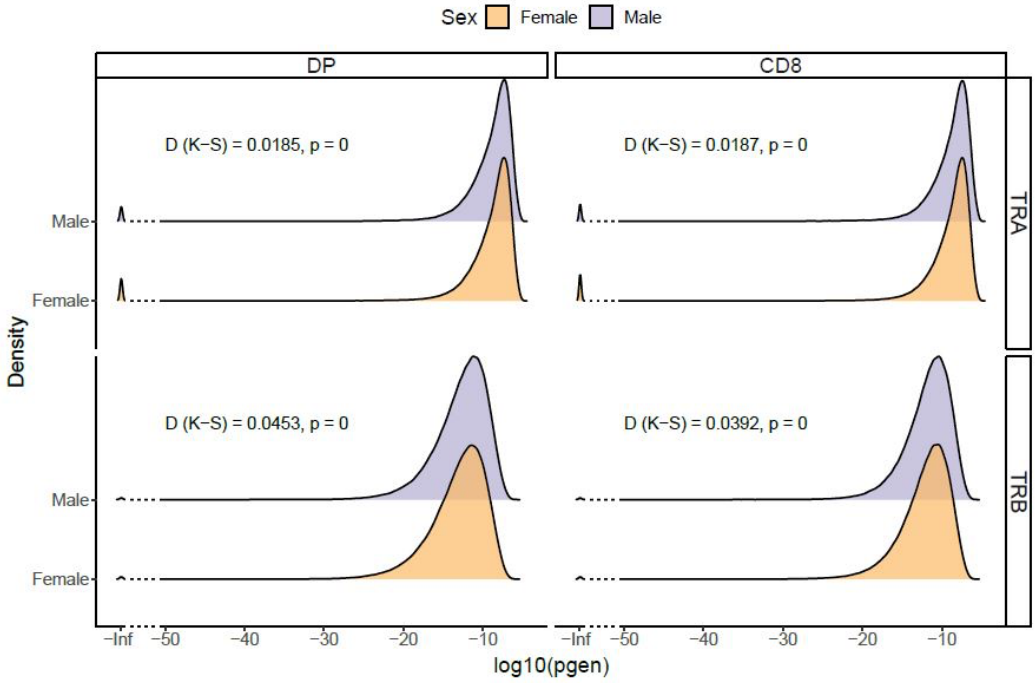

Figure 5: Probabilities of generation of TCRs in males and females.

The figure shows the distribution of Pgen (probability of generation) sequences between males and females for TRA and TRB in DP and CD8 cells. A V(D)J recombination model was created using 400,000 non-productive random sequences derived from the nonproductive sequences of all individuals for each chain, both for DP and CD8 cells (65). This model was then used to calculate the Pgen of sequences for each individual (66). The overall distribution comparison between males and females was tested using the Kolmogorov-Smirnov test, with the D value and associated p-value indicated. Males are depicted in violet and females in orange.

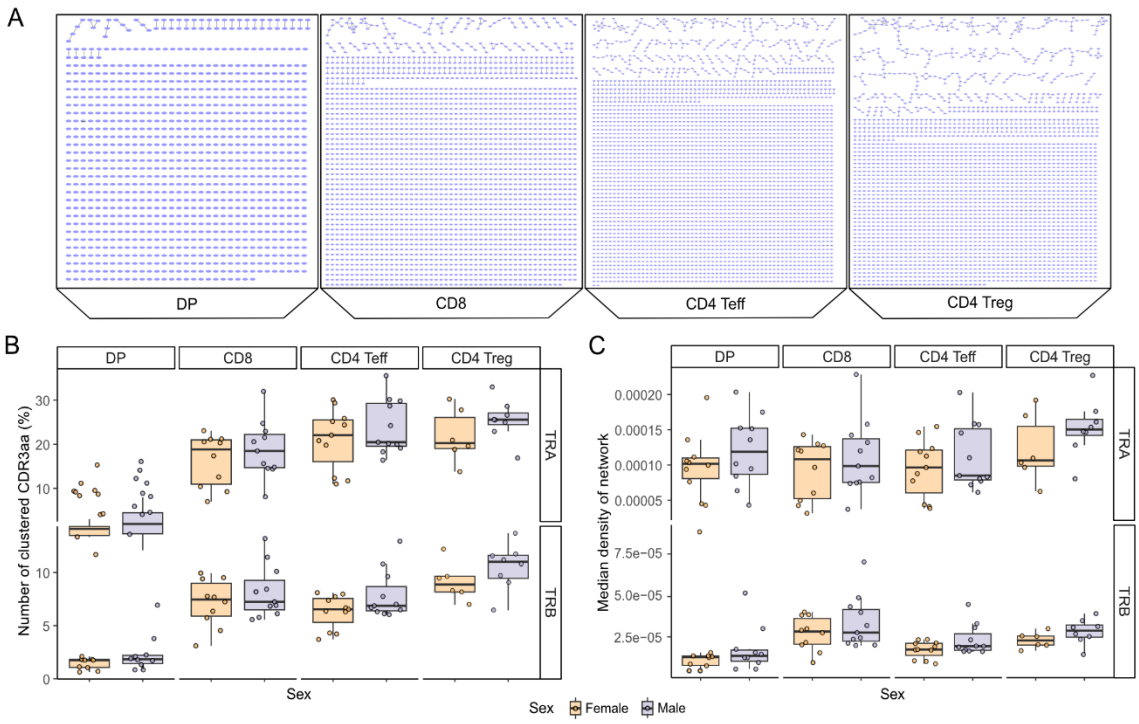

Figure 6: Comparable TCR repertoire network structure based on CDR3 amino acid sequence similarity between males and females. For each sample, 100 random subsamplings were performed on the minimum number of CDR3aa per cell subtype. Two CDR3aa are linked if they have a Levenshtein distance of one. **(A)** TRA Network structure of subsampled TCR repertoire of a male subject for DP, CD8, CD4 Teff and CD4 Treg SP (from left to right). Each point on the graph represents a CDR3aa. **(B-C)** Comparison of the proportion of linked sequences **(B)** and network density **(C)** between male and female samples, in DP (N = 22), CD8 (N = 23), CD4 Teff (N = 24) and CD4 Treg (N = 14). Each point on the graph represents the median value from 100 subsampling iterations for each sample. Statistical analysis using the Wilcoxon test revealed no significant sex differences for these two metrics ($p > 0.05$). Males are depicted in violet; females in orange.

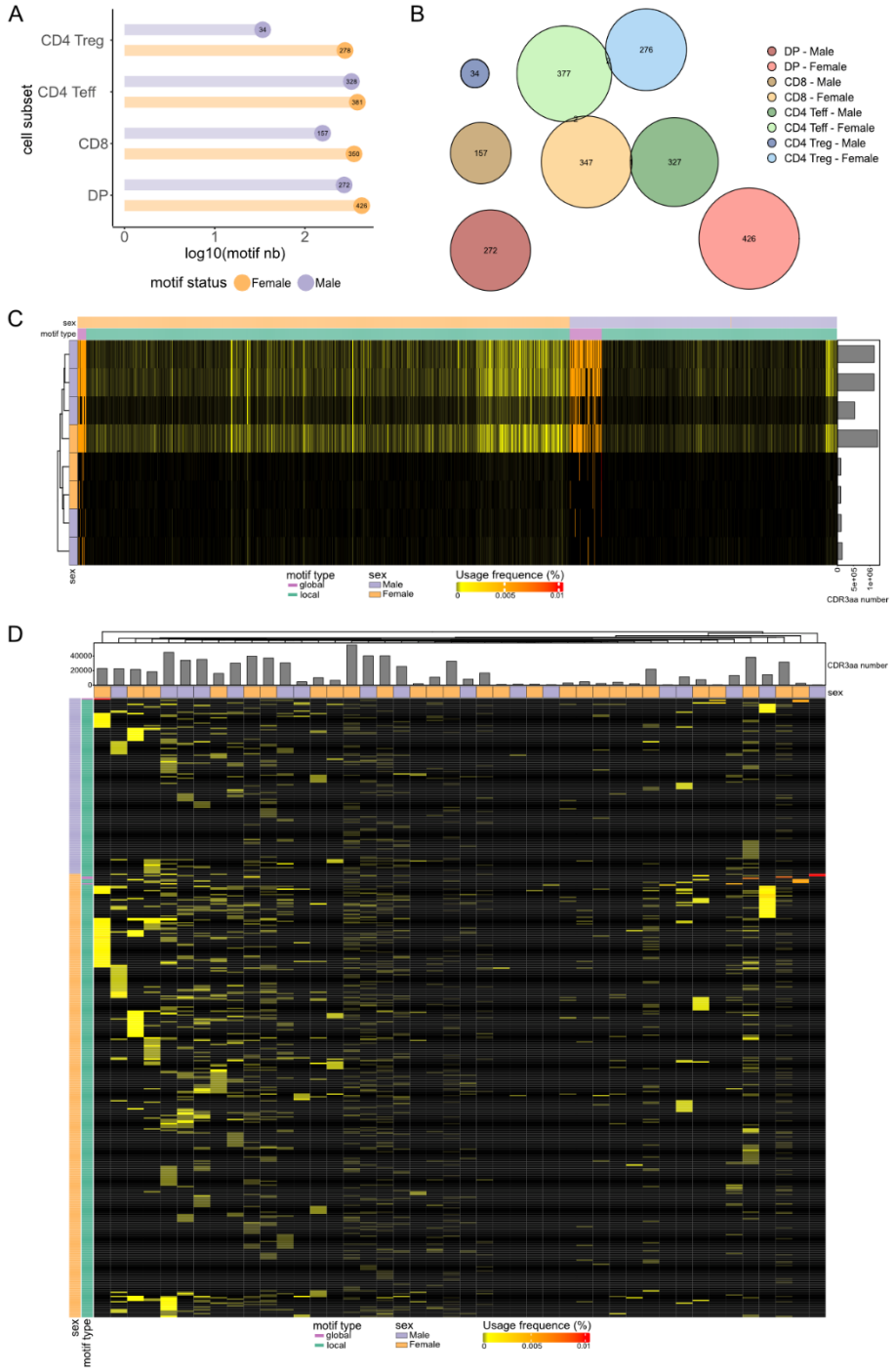

Figure 7: Thymic TRB TCR sex-associated motifs.

Different structural motifs found differentially expressed between males and females in our dataset. We distinguish local motifs as distinct aa sequences, and global motifs as motif regions with one variable aa position maintaining a BLOSUM62 score of ≥ 0. **(A)** Number of male and female associated motifs by cell subset. **(B)** Euler diagram illustrating the distribution and overlap between all sex-associated motifs. The numbers indicate the number of motifs in overlap zones. **(C-D)** Validation of these sex-associated TRB CDR3aa motifs. The following heatmap illustrates the usage of all the TRB CDR3aa motif in the external thymic pediatric dataset (35,36) **(C)** and those of TRB CD8 in the peripheral dataset **(D)**. Sex and total CDR3aa number are depicted by sample. Males are depicted in violet and females in orange then local motifs in blue-green and global motifs in magenta.

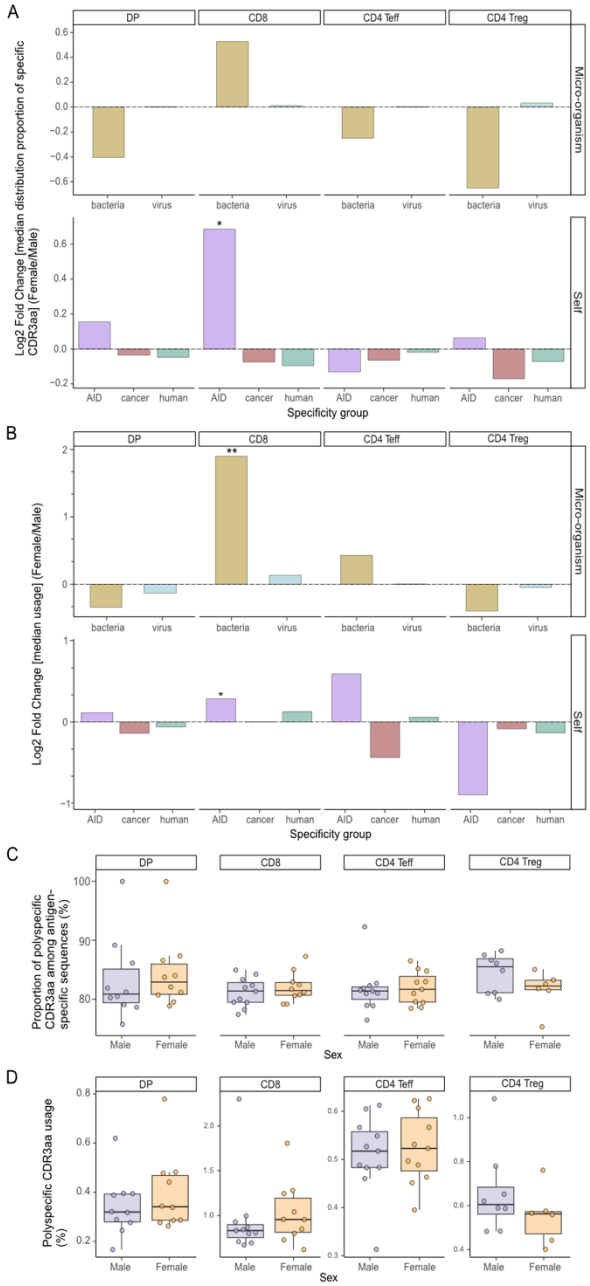

Figure 8: Sex-biased enrichment of TCRs specific for known antigens.
From a pooled and curated database, an exact match with this database infers the specificity of TRB CDR3aa of our thymic dataset. Many specificity groups are defined according to the nature of the antigen peptide targeted (bacteria, virus, autoimmune disease [AID], cancer and self-peptide no associated to disease [human]). This analysis compares the distributions of the proportion of unique TRB CDR3aa sequences with a specific specificity **(A)** and their usage **(B)** between females and males across cell subtypes, using the log2 fold change of the median values (females over males), following each specificity group. These groups of specificity are additionally classified as microorganism in the top section (bacteria in gold and virus in light blue) and self at the bottom (AID in magenta, cancer in red, human in blue-green). Polyspecific CDR3aa are defined here as CDR3aa capable of recognizing multiple antigens from different organisms (for no self-antigens) or from different specificity groups (e.g. categorized microorganisms, categorized self-antigens, allergens…). The proportion of polyspecific CDR3aa among antigen-specific sequences **(C)** and their usage **(D)** is compared between males and females, in DP (N = 22), CD8 (N = 23), CD4 Teff (N = 24) and CD4 Treg (N = 14) cells. Stars indicate statistical differences between males and females based on the p-value of the Wilcoxon test (*: $p < 0.05$, **: $p < 0.01$). Males are depicted in violet and females in orange.

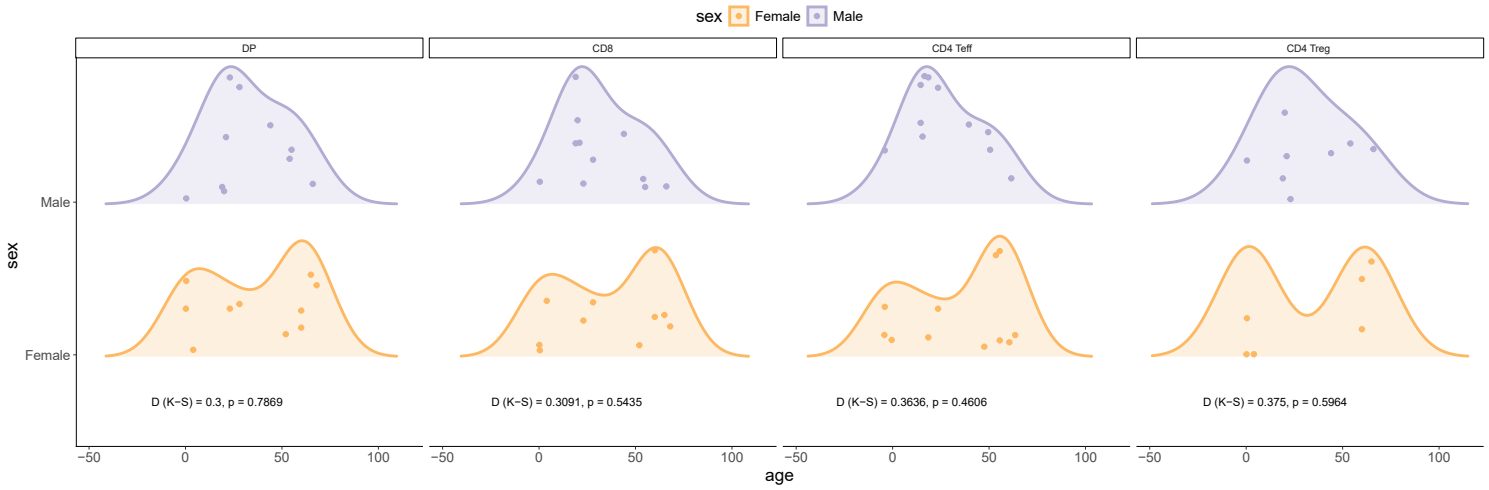
sex
Female
Male
DP
CD8
CD4 Teff
CD4 Treg
Male
Female
sex
D (K−S) = 0.3, p = 0.7869
D (K−S) = 0.3091, p = 0.5435
D (K−S) = 0.3636, p = 0.4606
D (K−S) = 0.375, p = 0.5964
−50
0
50
100
age

Supplemental Figure 1: Age distribution of male and female donors is comparable across thymic subsets.

Age of individual donors plotted separately for females (orange) and males (violet) for each thymic cell subset: double-positive (DP) thymocytes, CD8 single-positive (CD8), CD4 effector single-positive (CD4 Teff) and CD4 regulatory T-cell single-positive (CD4 Treg). For each subset, a two-sample Kolmogorov–Smirnov (K-S) test was performed; the D statistic and corresponding p-value are displayed below each panel. In all cases, no significant difference was detected, indicating balanced age distributions between sexes for every subset.

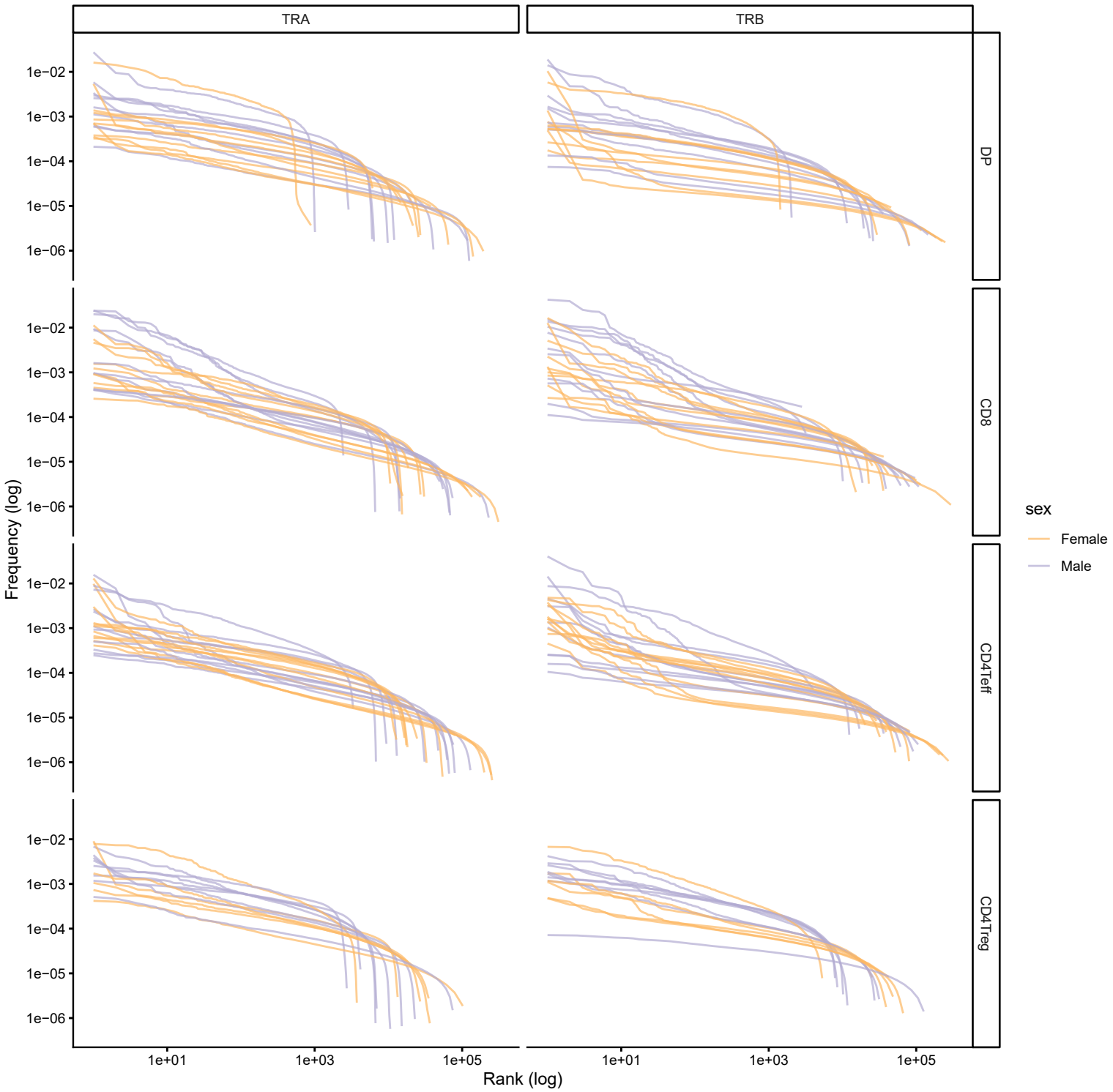
TRA
TRB
DP
CD8
CD4Teff
CD4Treg
Frequency (log)
1e−02
1e−03
1e−04
1e−05
1e−06
1e+01
1e+03
1e+05
Rank (log)
sex
Female
Male

Supplemental Figure 2: Rank–frequency distributions of thymic TRA and TRB clonotypes. Log–log rank–frequency plots of unique TRA (left) and TRB (right) clonotypes are shown for each donor and thymic subset (DP, CD8, CD4 Teff, CD4 Treg, from top to bottom). For each sample, clonotypes are ranked by decreasing abundance (x-axis, log scale), and their corresponding relative frequencies are plotted (y-axis, log scale). Curves display broadly comparable shapes across donors, with no obvious systematic differences between males and females, indicating similar clonotype abundance distributions and sampling depth across sexes.

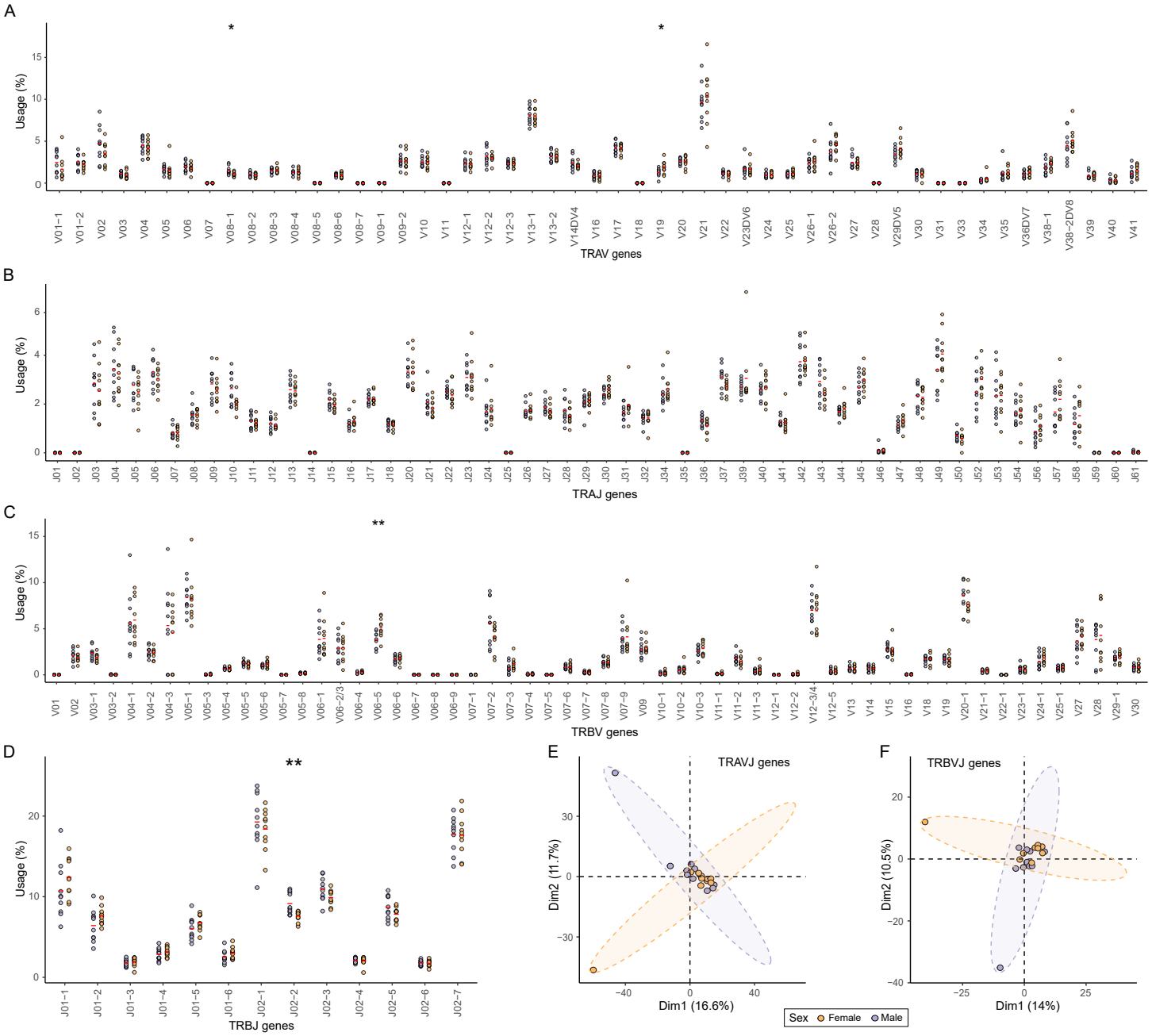
A
Usage (%)
TRAV genes
B
Usage (%)
TRAJ genes
C
Usage (%)
TRBV genes
D
Usage (%)
TRBJ genes
E
TRAVJ genes
Dim1 (16.6%)
Dim2 (11.7%)
F
TRBVJ genes
Dim1 (14%)
Dim2 (10.5%)
Sex
Female
Male

Supplemental Figure 3: Some differential V and J gene usage in TCR repertoires of DP cells between males and females.

(A-D) Frequencies of TRAV **(A)**, TRAJ **(B)**, TRBV **(C)**, and TRBJ **(D)** gene usage between males and females. Red lines represent the mean for each sex group. Statistical comparisons between groups were performed using the Wilcoxon test. Stars indicate statistical differences between males and females based on the p-value of the test (*: $p < 0.05$, **: $p < 0.01$). **(E-F)** Principal Component Analysis (PCA) derived from the distribution of the frequency of usage of TRAV-TRAJ **(E)** and TRBV-TRBJ **(F)** gene associations across sex groups between males and females. Each point represents an individual. Ellipses show 95% confidence intervals. Males are depicted in violet and females in orange.

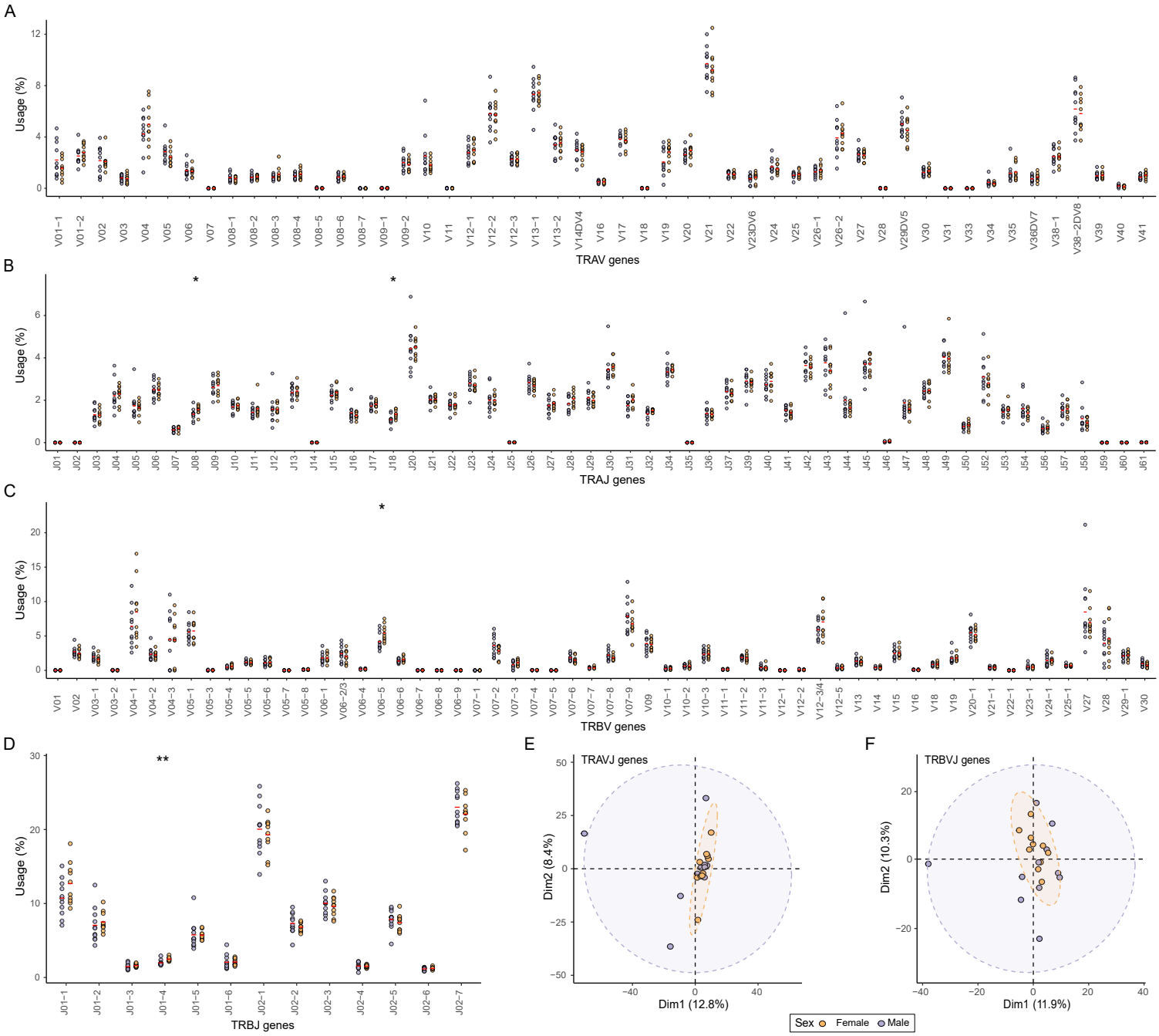
A
Usage (%)
TRAV genes
B
Usage (%)
TRAJ genes
C
Usage (%)
TRBV genes
D
Usage (%)
TRBJ genes
E
TRAVJ genes
Dim1 (12.8%)
Dim2 (8.4%)
F
TRBVJ genes
Dim1 (11.9%)
Dim2 (10.3%)
Sex
Female
Male

Supplemental Figure 4: Some differential V and J gene usage in TCR repertoires of CD8 cells between males and females.

(A-D) Frequencies of TRAV **(A)**, TRAJ **(B)**, TRBV **(C)**, and TRBJ **(D)** gene usage between males and females. Red lines represent the mean for each sex group. Statistical comparisons between groups were performed using the Wilcoxon test. Stars indicate statistical differences between males and females based on the p-value of the test (*: $p < 0.05$, **: $p < 0.01$). **(E-F)** Principal Component Analysis (PCA) derived from the distribution of the frequency usage of TRAV-TRAJ **(E)** and TRBV-TRBJ **(F)** gene associations across sex groups between males and females. Each point represents an individual. Ellipses show 95% confidence intervals. Males are depicted in violet and females in orange.

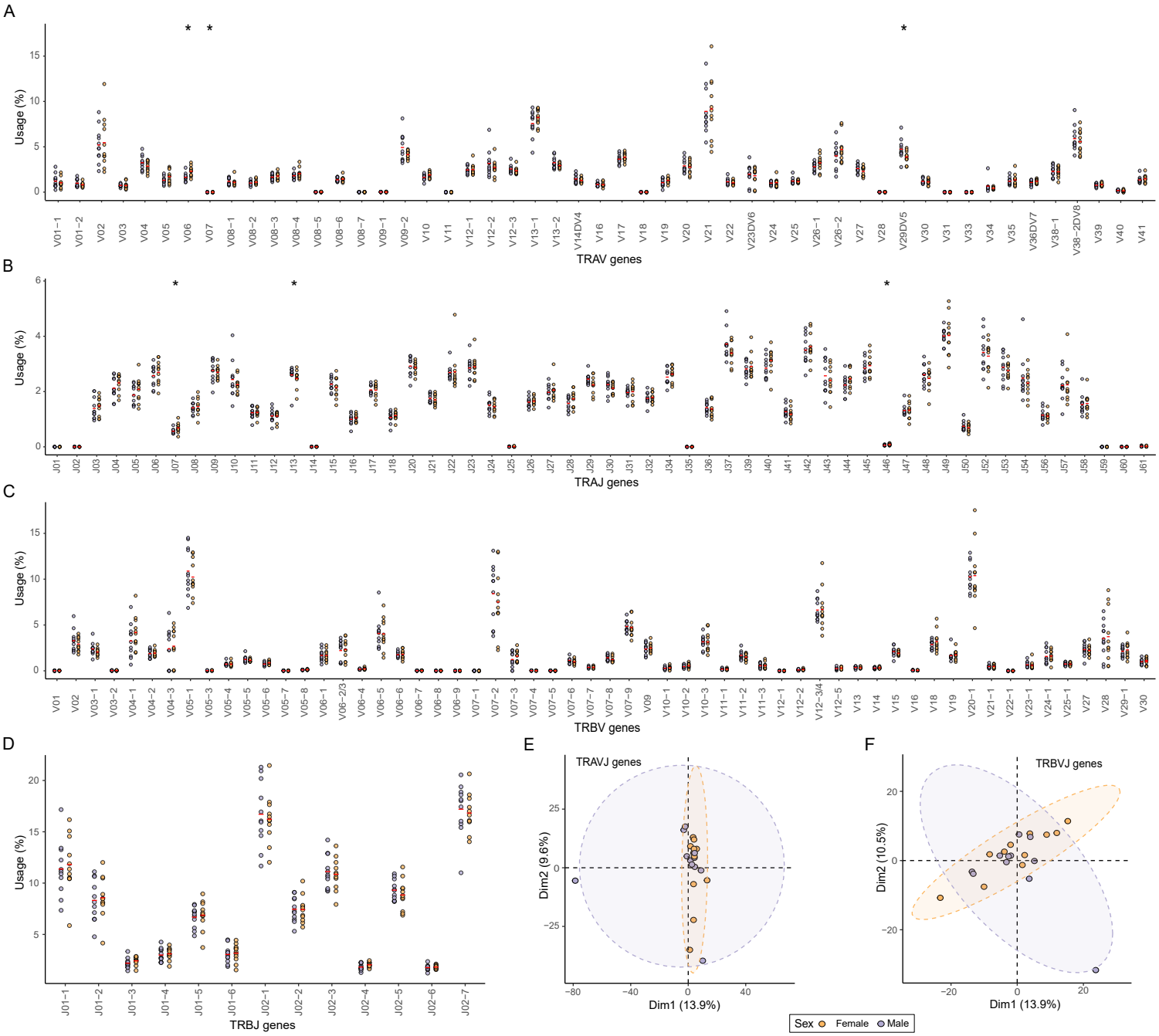
A
Usage (%)
TRAV genes
B
Usage (%)
TRAJ genes
C
Usage (%)
TRBV genes
D
Usage (%)
TRBJ genes
E
TRAVJ genes
Dim2 (9.6%)
Dim1 (13.9%)
F
TRBVJ genes
Dim2 (10.5%)
Dim1 (13.9%)
Sex
Female
Male

Supplemental Figure 5: Some differential V and J gene usage in TCR repertoires of CD4 Teff cells between males and females.

(A-D) Frequencies of TRAV **(A)**, TRAJ **(B)**, TRBV **(C)**, and TRBJ **(D)** gene usage between males and females. Red lines represent the mean for each sex group. Statistical comparisons between groups were performed using the Wilcoxon test. Stars indicate statistical differences between males and females based on the p-value of the test (*: $p < 0.05$, **: $p < 0.01$). **(E-F)** Principal Component Analysis (PCA) derived from the distribution of the frequency usage of TRAV-TRAJ **(E)** and TRBV-TRBJ **(F)** gene associations across sex groups between males and females. Each point represents an individual. Ellipses show 95% confidence intervals. Males are depicted in violet and females in orange.

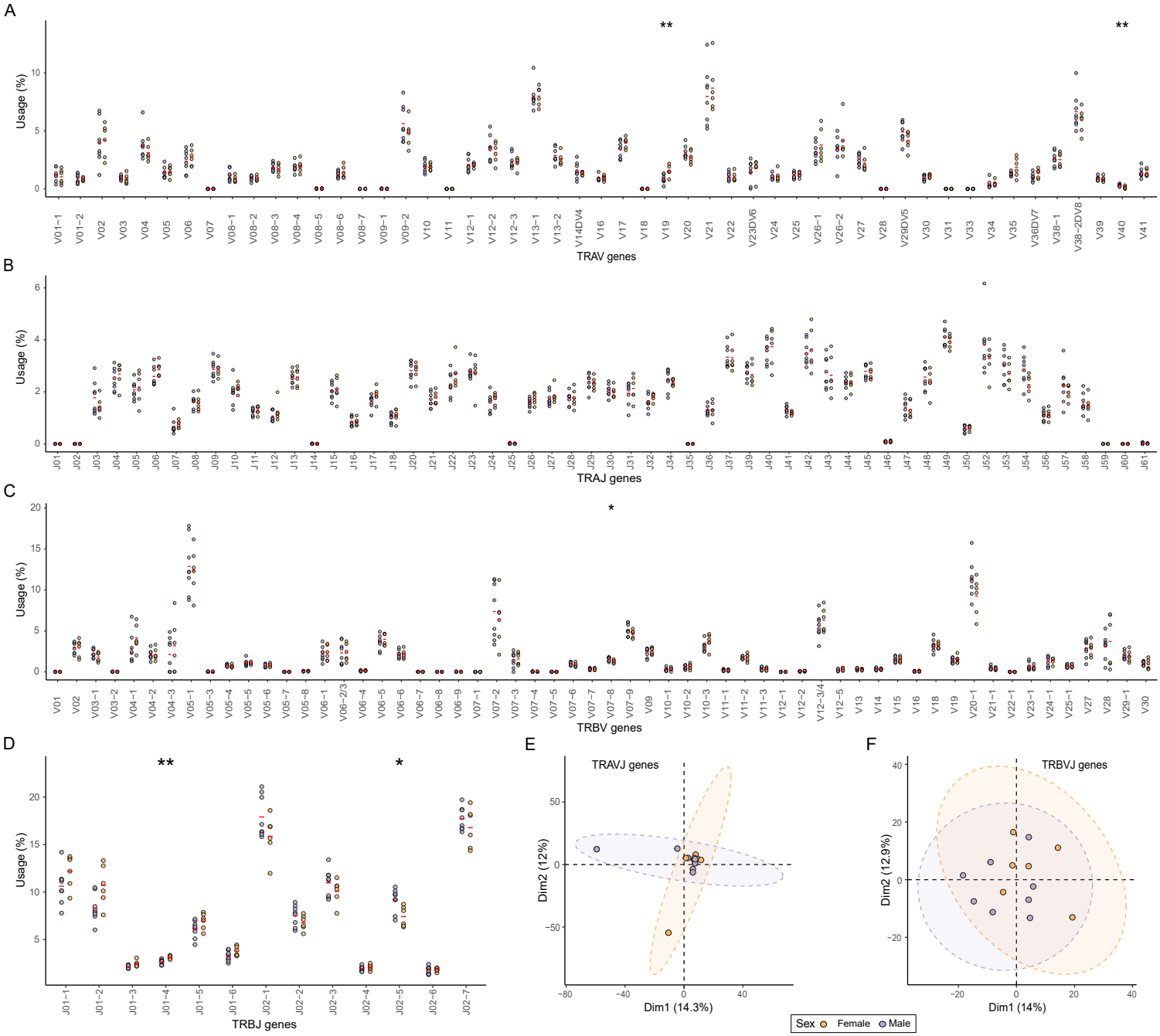
A
Usage (%)
TRAV genes
B
Usage (%)
TRAJ genes
C
Usage (%)
TRBV genes
D
Usage (%)
TRBJ genes
E
TRAVJ genes
Dim2 (12%)
Dim1 (14.3%)
F
TRBVJ genes
Dim2 (12.9%)
Dim1 (14%)
Sex Female Male

Supplemental Figure 6: Some differential V and J gene usage in TCR repertoires of CD4 Treg cells between males and females.

(A-D) Frequencies of TRAV **(A)**, TRAJ **(B)**, TRBV **(C)**, and TRBJ **(D)** gene usage between males and females. Red lines represent the mean for each sex group. Statistical comparisons between groups were performed using the Wilcoxon test. Stars indicate statistical differences between males and females based on the p-value of the test (*: $p < 0.05$, **: $p < 0.01$). **(E-F)** Principal Component Analysis (PCA) derived from the distribution of the usage frequency of TRAV-TRAJ **(E)** and TRBV-TRBJ **(F)** gene associations across sex groups between males and females. Each point represents an individual. Ellipses show 95% confidence intervals. Males are depicted in violet and females in orange.

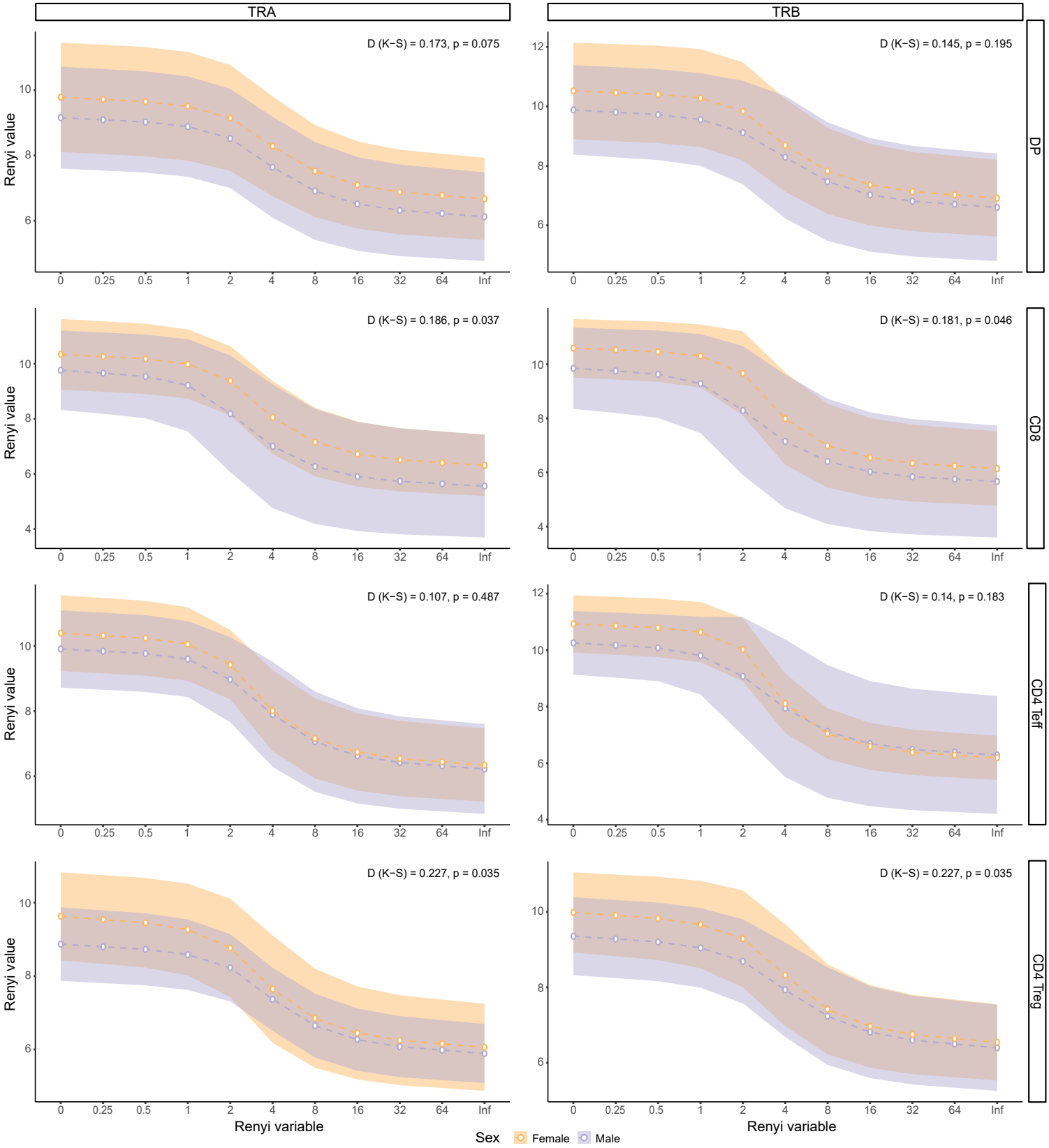
TRA
TRB
DP
CD8
CD4 Teff
CD4 Treg
D (K−S) = 0.173, p = 0.075
D (K−S) = 0.145, p = 0.195
D (K−S) = 0.186, p = 0.037
D (K−S) = 0.181, p = 0.046
D (K−S) = 0.107, p = 0.487
D (K−S) = 0.14, p = 0.183
D (K−S) = 0.227, p = 0.035
D (K−S) = 0.227, p = 0.035
Renyi value
Renyi variable
0
0.25
0.5
1
2
4
8
16
32
64
Inf
Sex
Female
Male

Supplemental Figure 7: Minimal differences in diversity profile of CD8 and CD4 Treg thymic TCR repertoire between males and females.

Diversity profile with Rényi diversity index values (α ranging from 0 to infinity) for all cell subsets, both TRA (left) and TRB (right). Clonotypes of each sample were rarefied fifty times to their effective diversity number [i.e. $e^{Shannon\ index}$] and the median of their Rényi values was used for analysis. Dotted lines and points show the mean value for each sex group, while the shaded area represents the standard deviation for each sex group. The overall shape of the curves was compared statistically using the Kolmogorov-Smirnov test, with the D value and associated p-value indicated.

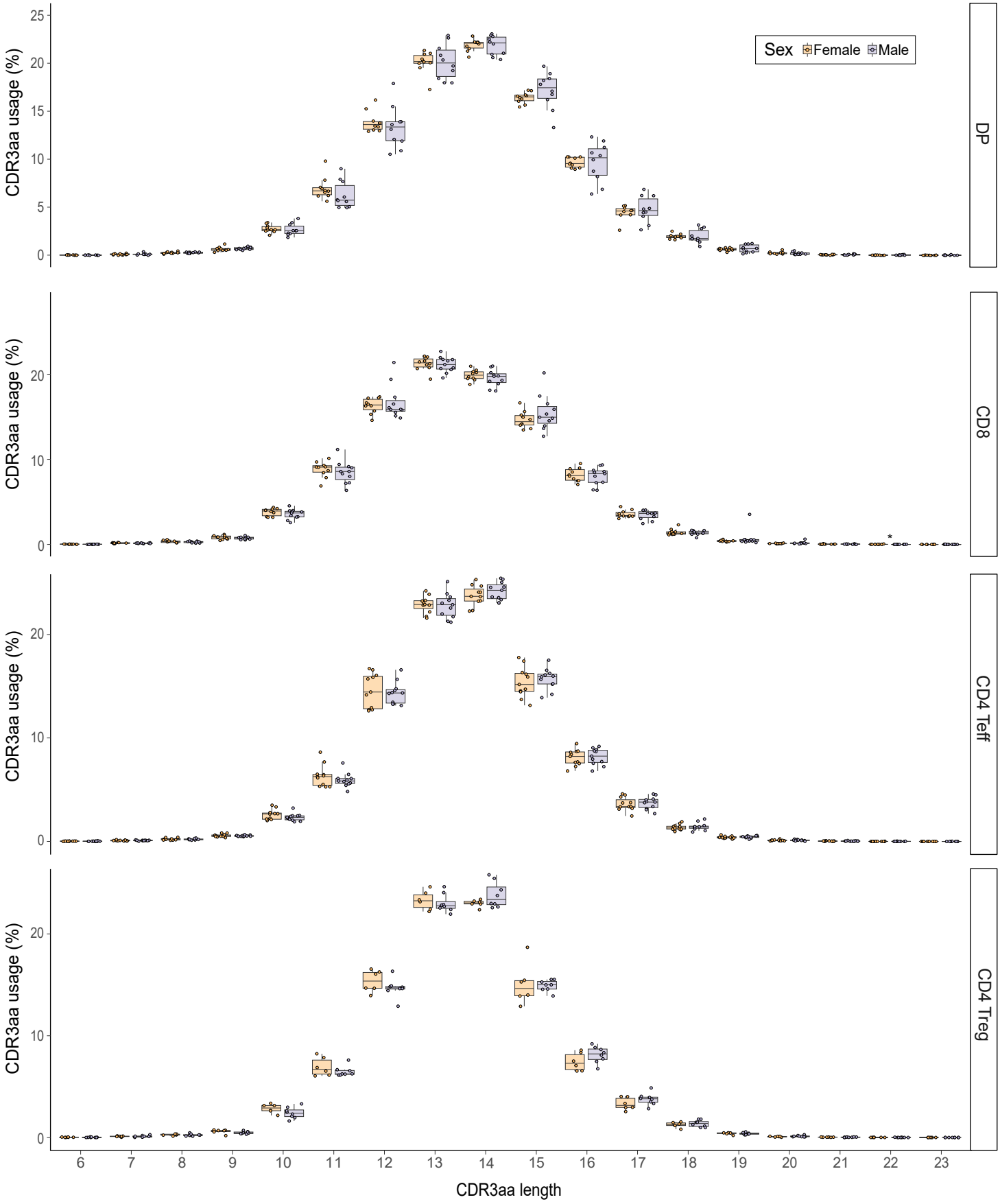
Sex
Female
Male
DP
CD8
CD4 Teff
CD4 Treg
CDR3aa usage (%)
CDR3aa length
0
5
10
15
20
25
6
7
8
9
10
11
12
13
14
15
16
17
18
19
20
21
22
23

Supplemental Figure 8: Comparable TRA CDR3aa length distribution between males and females. Distribution of CDR3aa length usage for TRA in all cell subsets. Stars indicate statistical differences between males and females based on the p-value of the Wilcoxon test (*: $p < 0.05$, **: $p < 0.01$). Males are depicted in violet and females in orange.

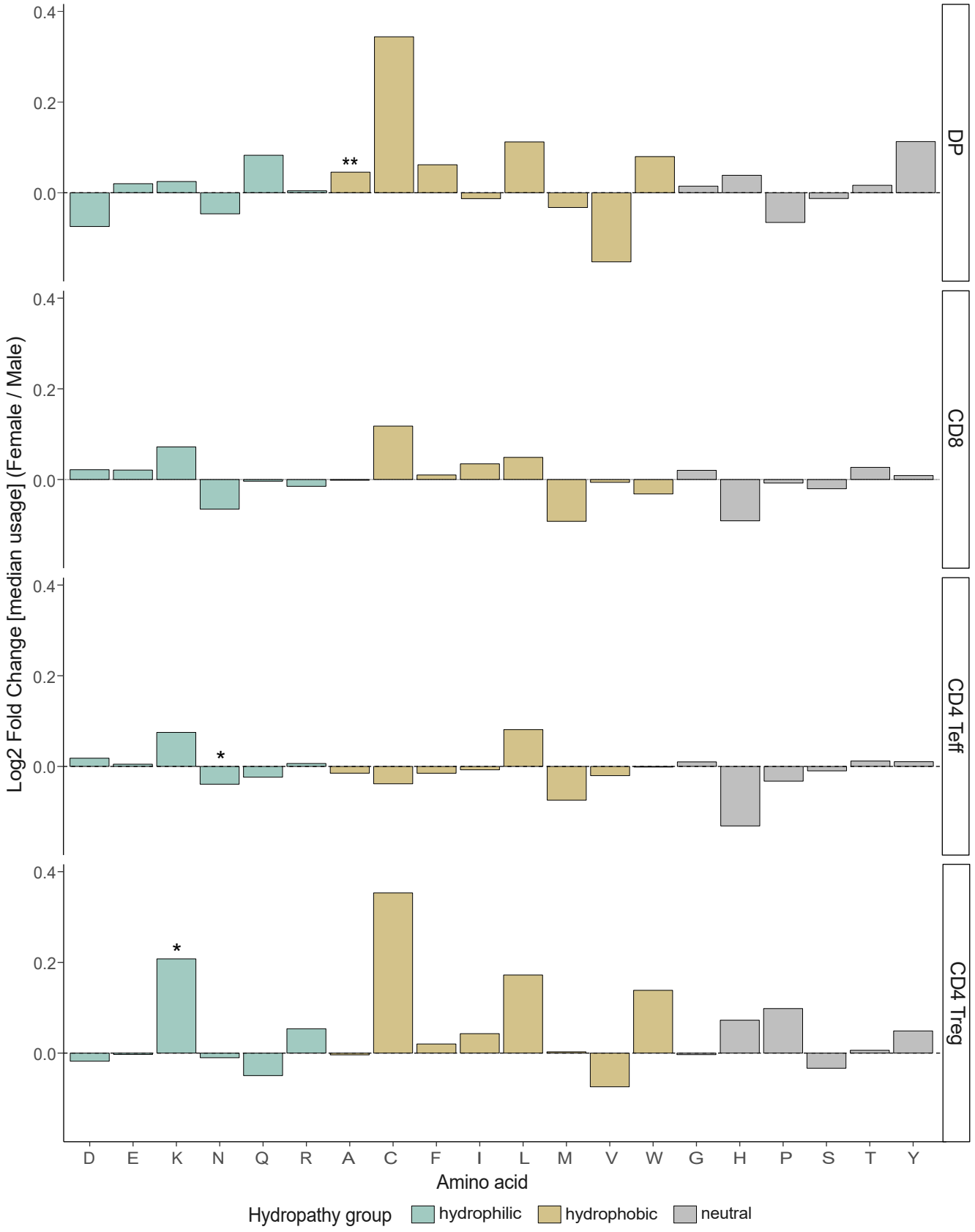
Log2 Fold Change [median usage] (Female / Male)
0.4
0.2
0.0
DP
CD8
CD4 Teff
CD4 Treg
**
*
*
D E K N Q R A C F I L M V W G H P S T Y
Amino acid
Hydropathy group
hydrophilic
hydrophobic
neutral

Supplemental Figure 9: Some differences in TRA CDR3aa usage between males and females.

Usage of each aa in the p108 to p114 CDR3 region represented as the log2 fold change of the median usage of females over males in TRA for each cell subset. A line at log2 fold change = 0 indicates the direction of the usage difference. Bars are colored according to the hydropathy class of the amino acid (neutral in gray, hydrophilic in blue-green and hydrophobic in gold). Stars indicate statistical differences between males and females based on the p-value of the Wilcoxon test (*: $p < 0.05$, **: $p < 0.01$).

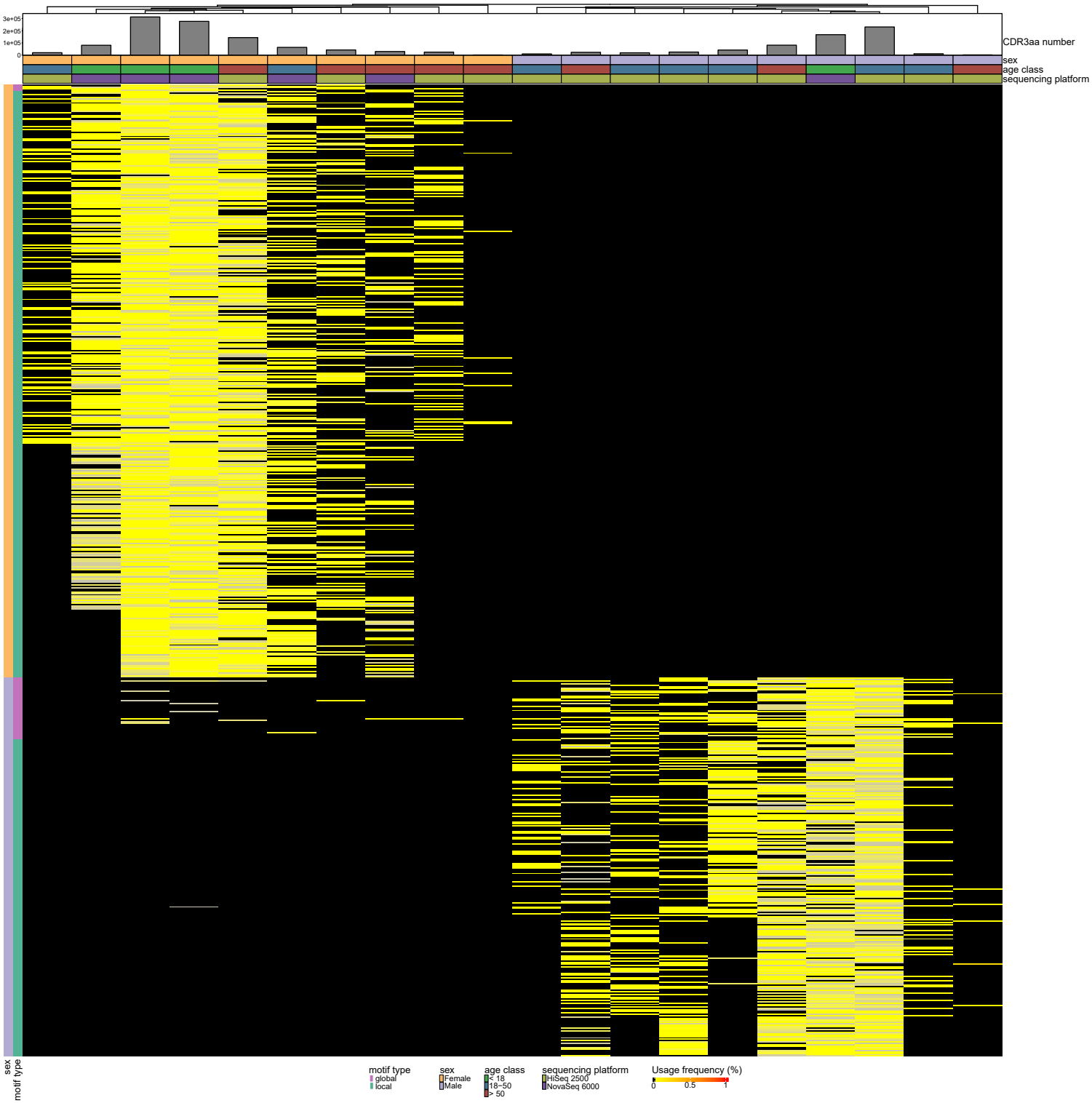
3e+05
2e+05
1e+05
0
CDR3aa number
sex
age class
sequencing platform
sex
motif type
motif type
global
local
sex
Female
Male
age class
< 18
18–50
> 50
sequencing platform
HiSeq 2500
NovaSeq 6000
Usage frequency (%)
0
0.5
1

Supplemental Figure 10: DP TRB thymic sex-associated motifs in our dataset.

Different structural motifs in the CDR3 amino acid (CDR3aa) region found differentially expressed between males and females within our dataset. Local motifs refer to distinct amino acid sequences, whereas global motifs represent motif regions with a single variable amino acid position maintaining a BLOSUM62 score ≥ 0. The heatmap showcases the differential usage of TRB CDR3aa motifs between males and females in of DP cells. Hierarchical clustering reveals clear segregation of individuals by sex, with most CDR3aa motifs being almost exclusively expressed in one sex while absent in the other. Sample attributes are visualized as follows: (1) Sex: males in violet, females in orange; (2) Age class: children (<18 years) in green, young adults (18-50 years) in blue, older adults (>50 years) in red; (3) sequencing platform: HiSeq2500 samples in persimmon, NovaSeq 6000 samples in purple; (4) the total CDR3aa number. Motifs overexpressed in males are shown in violet, those overexpressed in females in orange; local motifs are indicated in blue-green and global motifs in magenta.

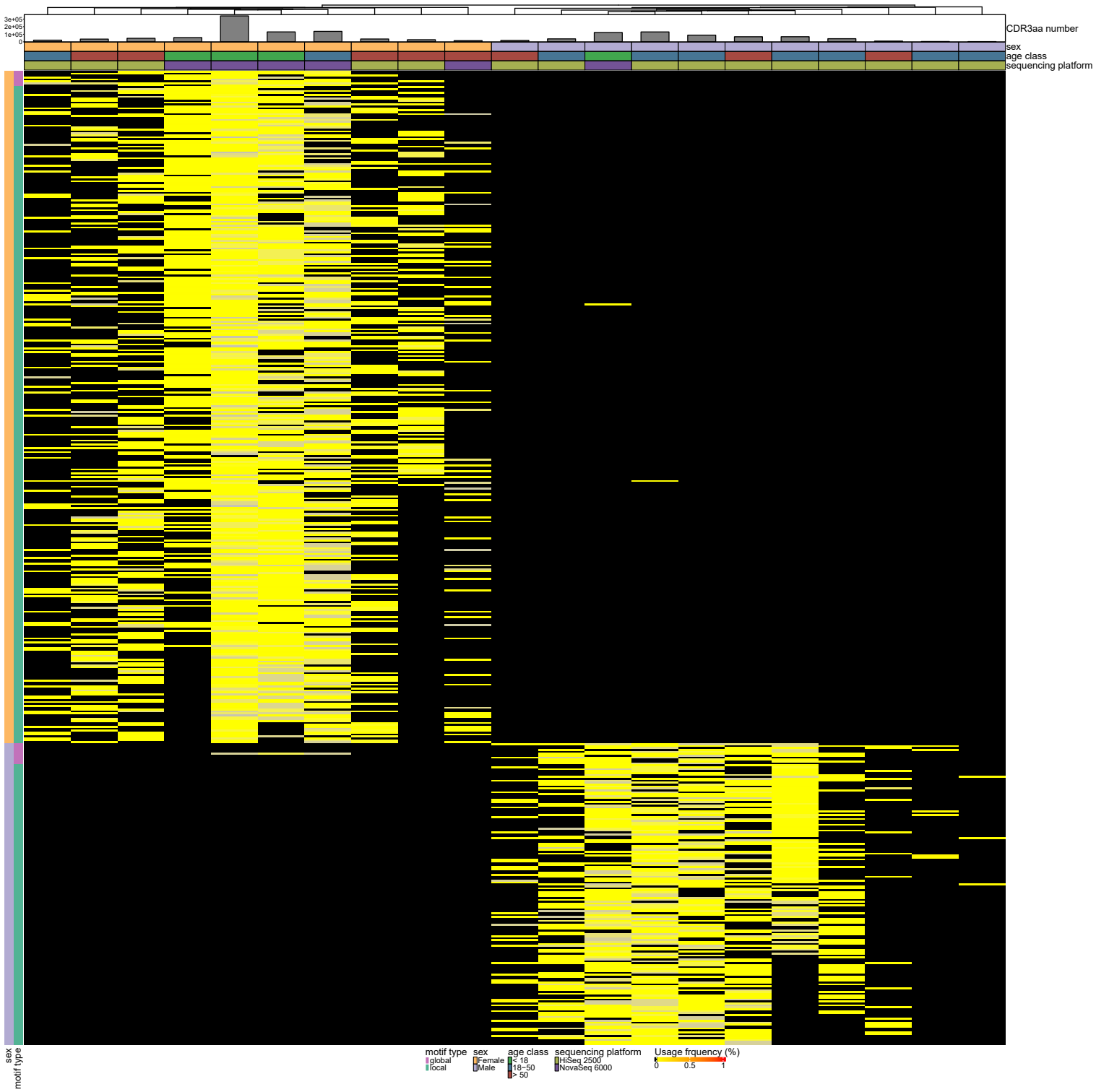
3e+05
2e+05
1e+05
0
CDR3aa number
sex
age class
sequencing platform
sex
motif type
motif type
global
local
sex
Female
Male
age class
< 18
18–50
> 50
sequencing platform
HiSeq 2500
NovaSeq 6000
Usage frquency (%)
0
0.5
1

Supplemental Figure 11: CD8 TRB thymic sex-associated motifs in our dataset.

Different structural motifs in the CDR3 amino acid (CDR3aa) region found differentially expressed between males and females within our dataset. Local motifs refer to distinct amino acid sequences, whereas global motifs represent motif regions with a single variable amino acid position maintaining a BLOSUM62 score ≥ 0. The heatmap showcases the differential usage of TRB CDR3aa motifs between males and females in of CD8 cells. Hierarchical clustering reveals clear segregation of individuals by sex, with most CDR3aa motifs being almost exclusively expressed in one sex while absent in the other. Sample attributes are visualized as follows: (1) Sex: males in violet, females in orange; (2) Age class: children (<18 years) in green, young adults (18-50 years) in blue, older adults (>50 years) in red; (3) sequencing platform: HiSeq2500 samples in persimmon, NovaSeq 6000 samples in purple; (4) the total CDR3aa number. Motifs overexpressed in males are shown in violet, those overexpressed in females in orange; local motifs are indicated in blue-green and global motifs in magenta.

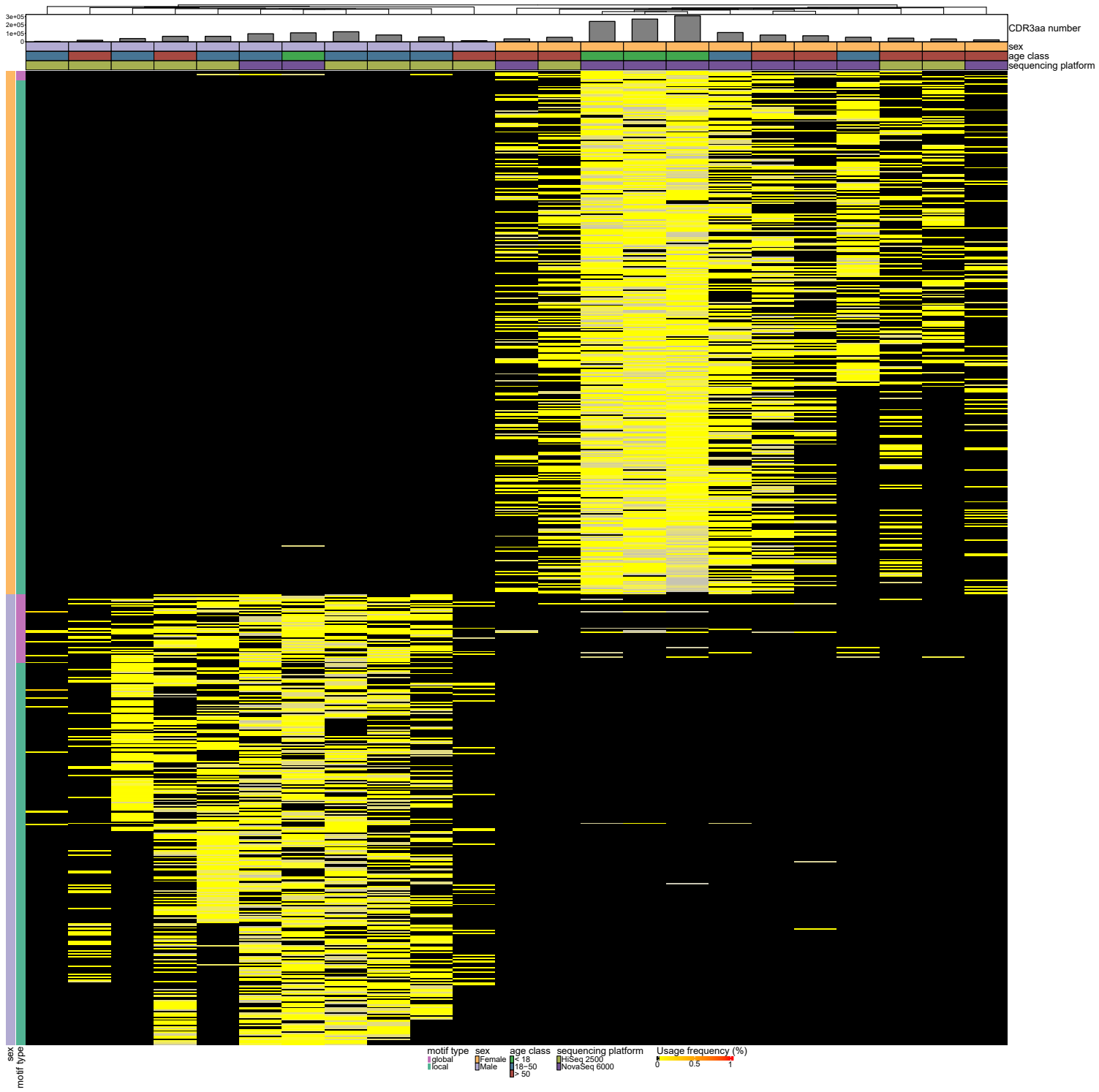
3e+05
2e+05
1e+05
0
CDR3aa number
sex
age class
sequencing platform
sex
motif type
motif type
global
local
sex
Female
Male
age class
< 18
18−50
> 50
sequencing platform
HiSeq 2500
NovaSeq 6000
Usage frequency (%)
0
0.5
1

Supplemental Figure 12: CD4 Teff TRB thymic sex-associated motifs in our dataset.

Different structural motifs in the CDR3 amino acid (CDR3aa) region found differentially expressed between males and females within our dataset. Local motifs refer to distinct amino acid sequences, whereas global motifs represent motif regions with a single variable amino acid position maintaining a BLOSUM62 score ≥ 0. The heatmap showcases the differential usage of TRB CDR3aa motifs between males and females in of CD4 Teff cells. Hierarchical clustering reveals clear segregation of individuals by sex, with most CDR3aa motifs being almost exclusively expressed in one sex while absent in the other. Sample attributes are visualized as follows: (1) Sex: males in violet, females in orange; (2) Age class: children (<18 years) in green, young adults (18-50 years) in blue, older adults (>50 years) in red; (3) sequencing platform: HiSeq2500 samples in persimmon, NovaSeq 6000 samples in purple; (4) the total CDR3aa number. Motifs overexpressed in males are shown in violet, those overexpressed in females in orange; local motifs are indicated in blue-green and global motifs in magenta.

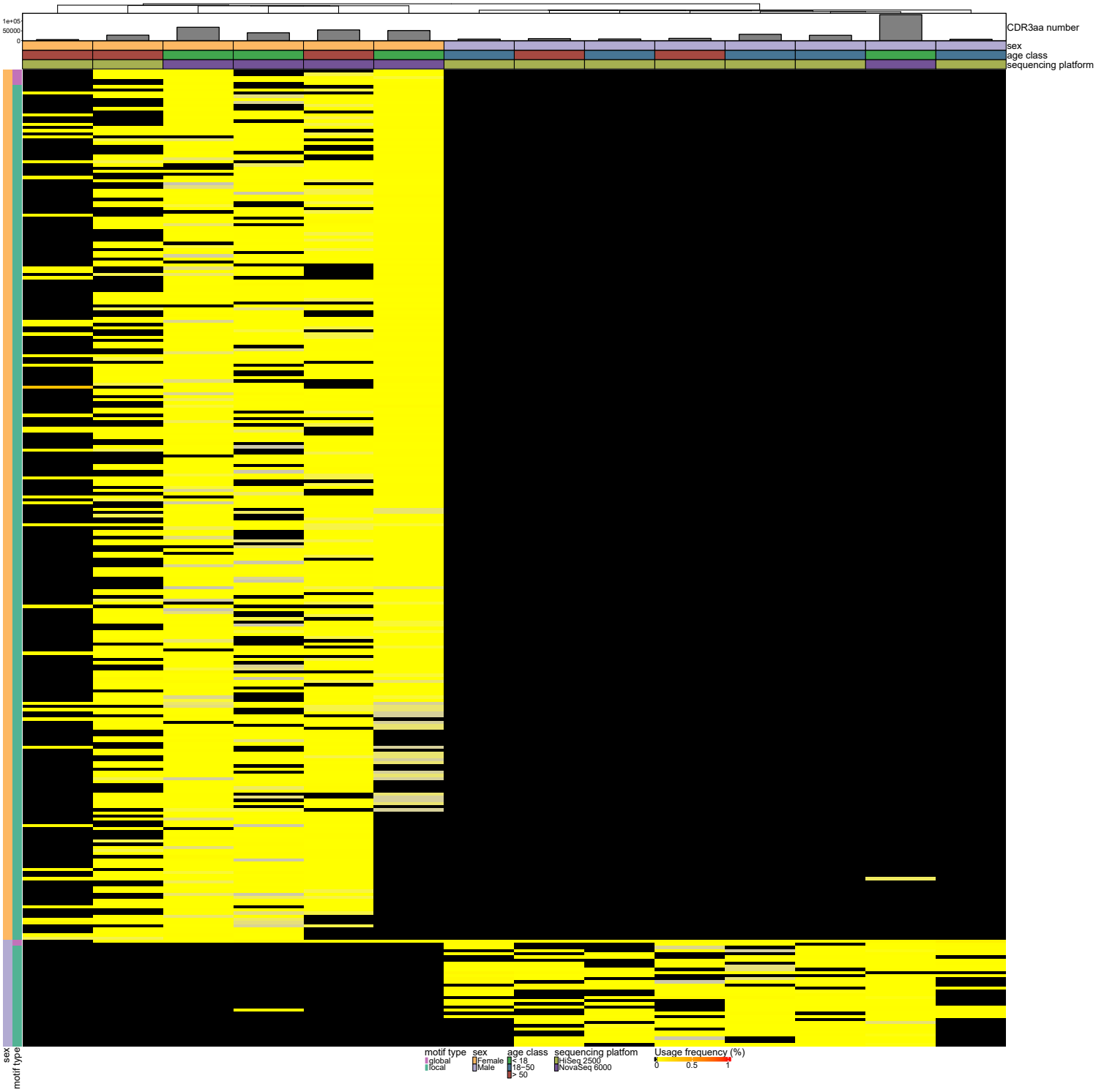
1e+05
50000
0
CDR3aa number
sex
age class
sequencing platform
sex
motif type
motif type
global
local
sex
Female
Male
age class
< 18
18−50
> 50
sequencing platfom
HiSeq 2500
NovaSeq 6000
Usage frequency (%)
0
0.5
1

Supplemental Figure 13: CD4 Treg TRB thymic sex-associated motifs in our dataset.

Different structural motifs in the CDR3 amino acid (CDR3aa) region found differentially expressed between males and females within our dataset. Local motifs refer to distinct amino acid sequences, whereas global motifs represent motif regions with a single variable amino acid position maintaining a BLOSUM62 score ≥ 0. The heatmap showcases the differential usage of TRB CDR3aa motifs between males and females in of CD4 Treg cells. Hierarchical clustering reveals clear segregation of individuals by sex, with most CDR3aa motifs being almost exclusively expressed in one sex while absent in the other. Sample attributes are visualized as follows: (1) Sex: males in violet, females in orange; (2) Age class: children (<18 years) in green, young adults (18-50 years) in blue, older adults (>50 years) in red; (3) sequencing platform: HiSeq2500 samples in persimmon, NovaSeq 6000 samples in purple; (4) the total CDR3aa number. Motifs overexpressed in males are shown in violet, those overexpressed in females in orange; local motifs are indicated in blue-green and global motifs in magenta.

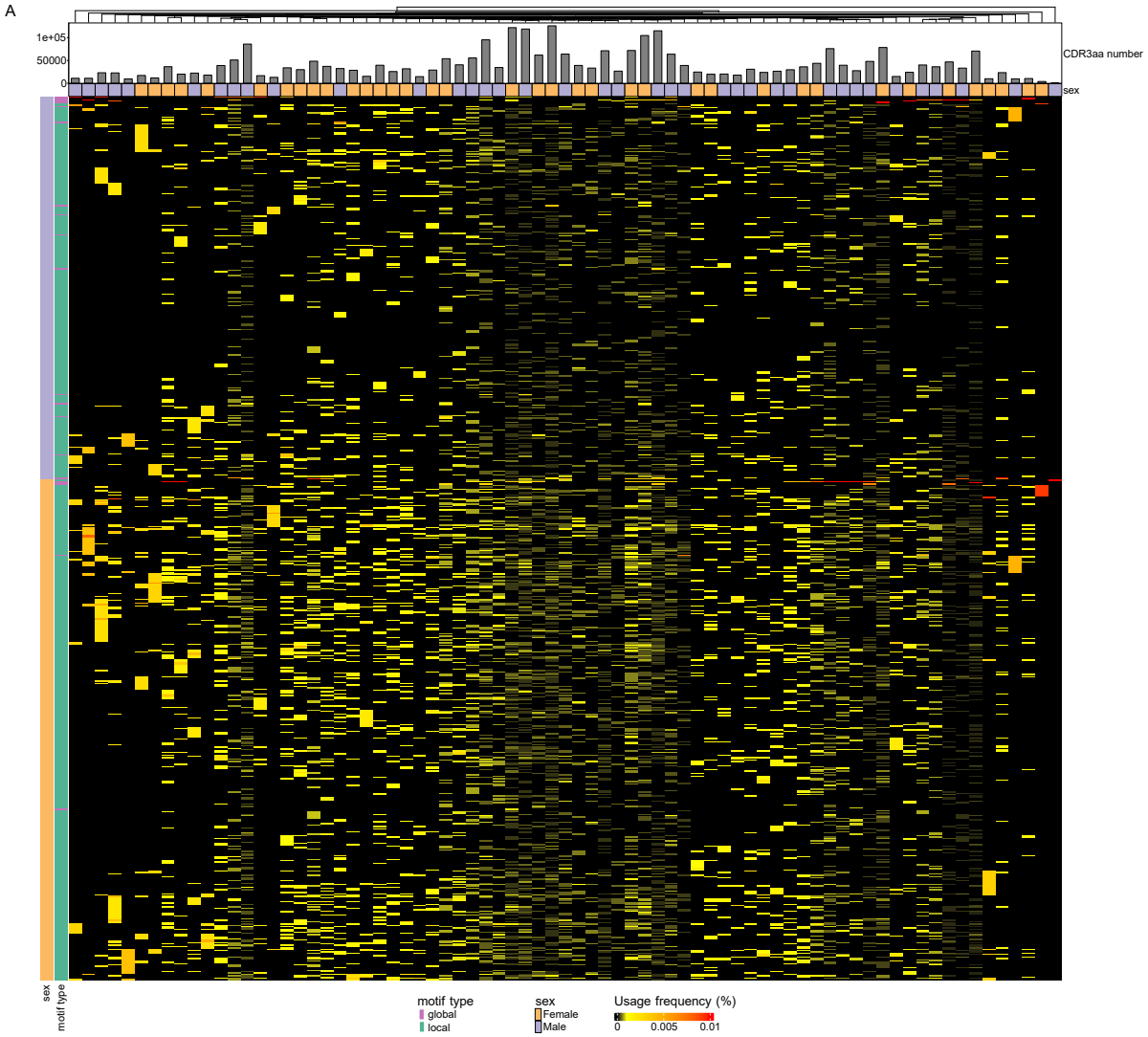
A
1e+05
50000
0
CDR3aa number
sex
sex
motif type
motif type
global
local
sex
Female
Male
Usage frequency (%)
0
0.005
0.01

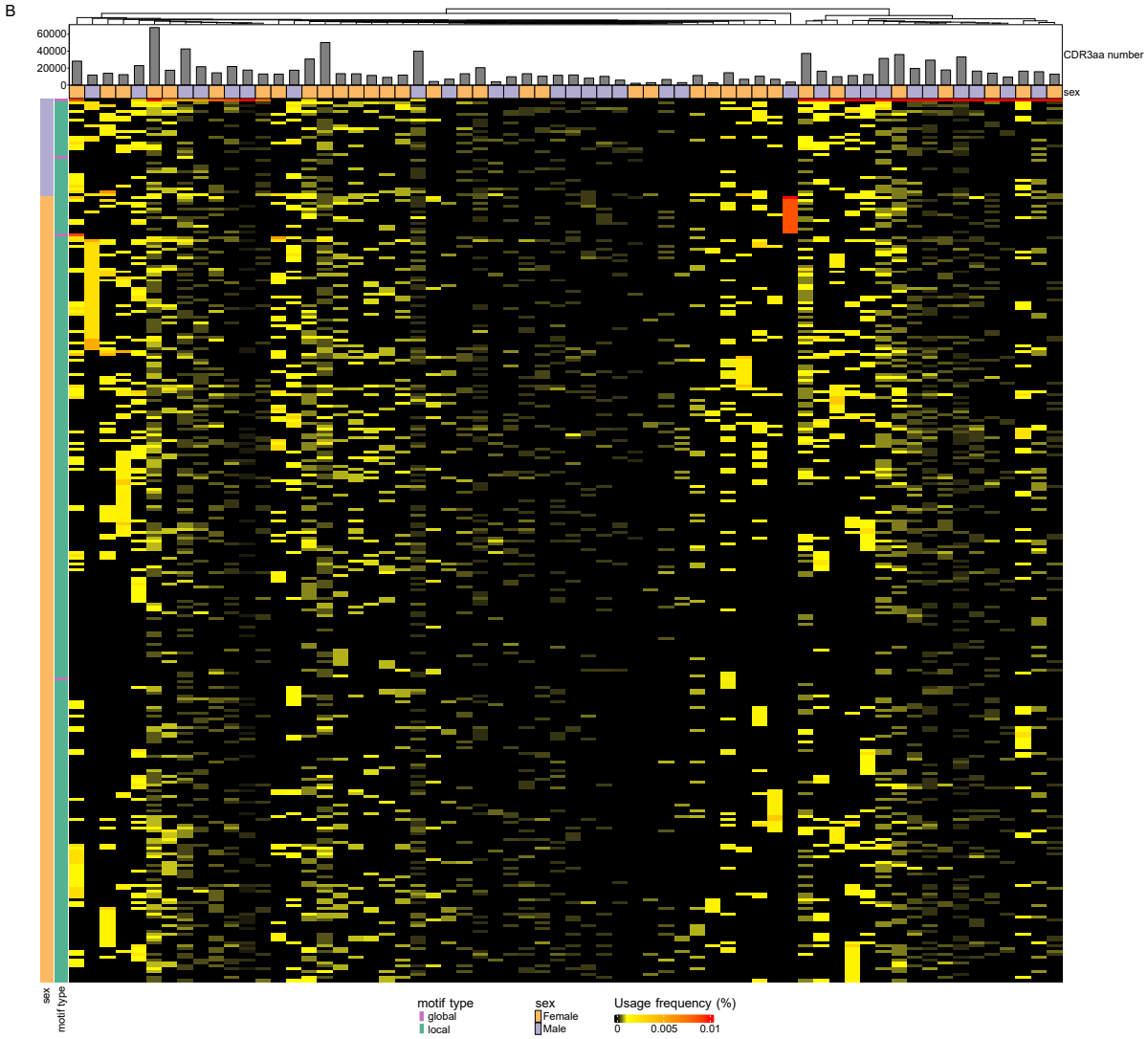
B
60000
40000
20000
0
CDR3aa number
sex
sex
motif type
motif type
global
local
sex
Female
Male
Usage frequency (%)
0
0.005
0.01

Supplemental Figure 14: TRB thymic sex associated motifs are not differentially expressed between males and females in peripheral TCR repertoire.

Heatmap representing TRB CDR3aa motif usage differentially expressed between males and females in CD4 Teff **(A)** and CD4 Treg **(B)** cells in a peripheral TCR repertoire dataset. Sex and total CDR3aa number are depicted by samples. Males are depicted in violet and females in orange and local motif in blue-green and global motifs in magenta.

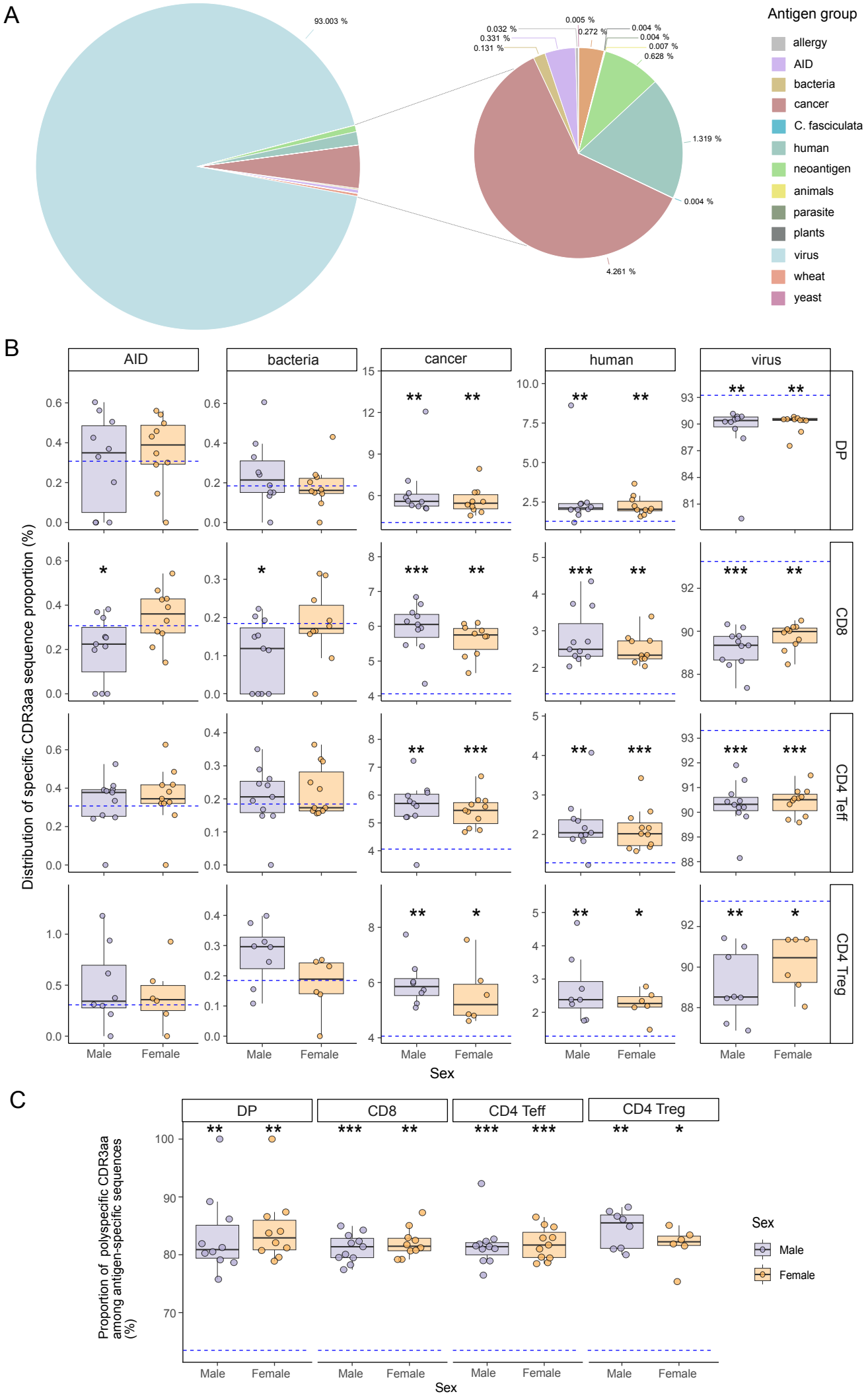
A
93.003 %
0.032 %
0.331 %
0.131 %
0.005 %
0.272 %
0.004 %
0.004 %
0.007 %
0.628 %
1.319 %
0.004 %
4.261 %
Antigen group
allergy
AID
bacteria
cancer
C. fasciculata
human
neoantigen
animals
parasite
plants
virus
wheat
yeast
B
AID
bacteria
cancer
human
virus
DP
CD8
CD4 Teff
CD4 Treg
Distribution of specific CDR3aa sequence proportion (%)
Male
Female
Sex
C
DP
CD8
CD4 Teff
CD4 Treg
Proportion of polyspecific CDR3aa among antigen-specific sequences (%)
Male
Female
Sex

Supplemental Figure 15: Enrichment of cancer associated, no-associated disease self-peptide specific and polyspecific TCRs, in our thymic dataset compared to initial curated database.

(A) Representation of the specificity groups in the pooled and curated database. **(B)** Distribution of specific CDR3aa sequence proportions for each sample across autoimmune disease (AID), bacteria, cancer, human and virus groups compared to the reference database distributions for males and females. **(C)** Proportion of polyspecific CDR3aa among antigen-specific sequences of samples compared to the reference database for both sexes. Stars indicate statistical significance between groups (males or females) and the pooled, curated database based on Wilcoxon test p-values (*: $p < 0.05$, **: $p < 0.01$). Males are depicted in violet and females in orange.

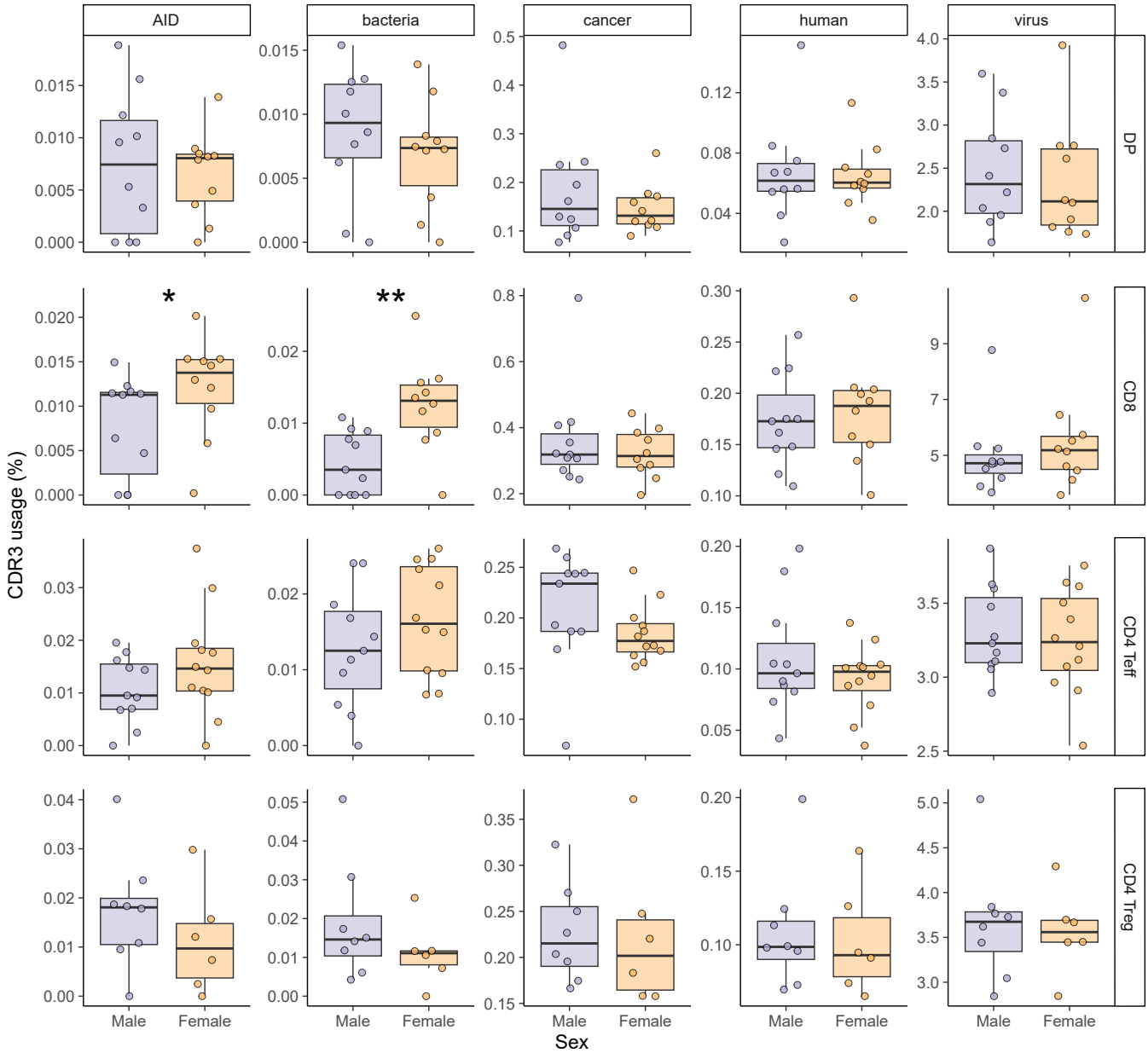
AID
bacteria
cancer
human
virus
DP
CD8
CD4 Teff
CD4 Treg
CDR3 usage (%)
Male
Female
Sex
*
**

Supplemental Figure 16: Enrichment of AID associated TCR and bacteria targeted TCR in CD8 female cells.

CDR3aa usage of CDR3aa with a specificity in autoimmunity disease, bacteria, cancer, human and virus groups. Stars indicate statistical differences between males and females based on the p-value of the Wilcoxon test (*: $p < 0.05$, **: $p < 0.01$). Males are depicted in violet and females in orange.

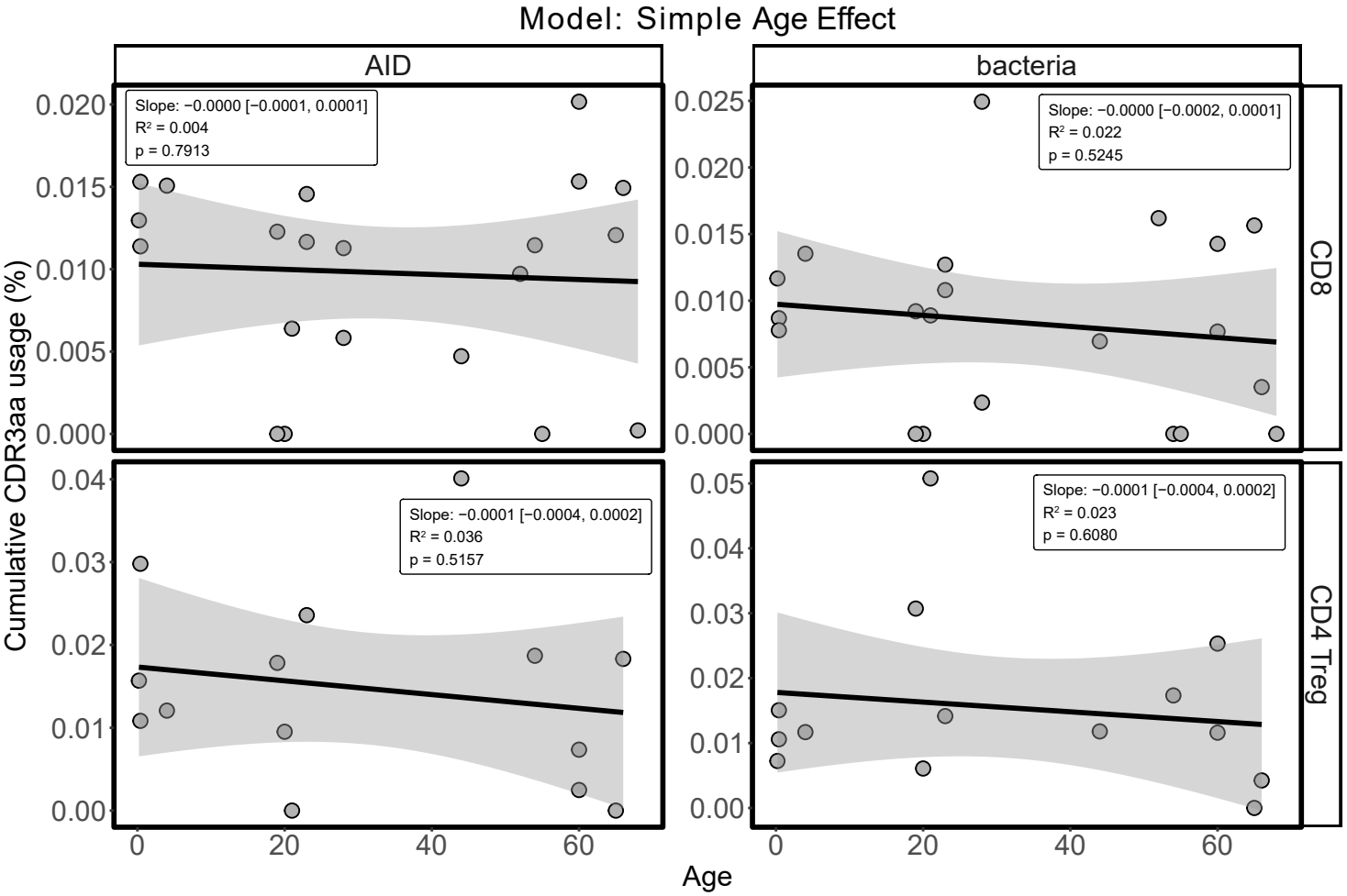
Model: Simple Age Effect
AID
bacteria
CD8
CD4 Treg
Slope: −0.0000 [−0.0001, 0.0001]
R² = 0.004
p = 0.7913
Slope: −0.0000 [−0.0002, 0.0001]
R² = 0.022
p = 0.5245
Slope: −0.0001 [−0.0004, 0.0002]
R² = 0.036
p = 0.5157
Slope: −0.0001 [−0.0004, 0.0002]
R² = 0.023
p = 0.6080
Cumulative CDR3aa usage (%)
Age

Supplemental Figure 17: No association between age and thymic usage of CDR3 sequences specific to autoimmunity or bacterial antigens.

Linear regression models assessing the effect of donor age on the cumulative usage (%) of TRB CDR3aa sequences with known specificity to self-antigens associated with autoimmunity (AID, left panels) or bacterial antigens (right panels), in CD8 SP (top) and CD4 Treg SP (bottom) thymic subsets. Each dot represents one donor. The shaded area indicates the 95% confidence interval around the regression line. Reported slope, 95% confidence interval, R^2, and p-values show no significant effect of age.

	DP cells	CD8 cells	CD4 Teff	CD4 Treg
TRA	1013	2433	3314	2654
TRB	1429	3496	4551	5383

Supplemental Table 1: Minimal number of CDR3aa by cell subset.